

Report LR-693

Development and Application of a Comprehensive, Design-sensitive Weight Prediction Method for Wing Structures of Transport Category Aircraft

September 1992

E. Torenbeek

Development and Application of a Comprehensive, Design-sensitive Weight Prediction Method for Wing Structures of Transport Category Aircraft

E. Torenbeek

Delft University of Technology
Department of Aerospace Engineering

Report LR-693

DEVELOPMENT AND APPLICATION OF A COMPREHENSIVE, DESIGN-
SENSITIVE WEIGHT PREDICTION METHOD FOR WING STRUCTURES OF
TRANSPORT CATEGORY AIRCRAFT

by prof.ir. E. Torenbeek

Delft, September 1992

SUMMARY

The present report describes the development of an analytical-empirical method to predict the structural weight of transport aircraft wings. The method is especially suitable for the preliminary design stage, when sensitivity studies are required of the effects of geometry and other variations on the design characteristics.

The wing weight is computed as the sum of several functional components, each of which is estimated via a rational approach and sometimes based on statistical evidence. The basic weight required to resist bending and shear loads is computed from integration of a spanwise material distribution. Weight penalties are derived for non-optimum effects, including stiffness required to cope with aeroelastic effects. Simple methods are derived for leading and trailing edge structures, including high-lift devices and control surfaces. Instead of using the suggested statistical data for mean stress levels, the user may input more accurate data, if available. This allows him to study alternative material applications or technologies such as Active Controls for Gust or Manoever Load Alleviation. The baseline is 1980+ technology.

Application of the method to several present-day transport aircraft illustrates its use and its accuracy. For the cases considered the prediction error was below 4 percent.

CONTENTS

	Page
Nomenclature	iv
1. Introduction	1
2. Weight subdivision, geometry and methodology	3
3. The bending moment due to lift	4
4. Material required to resist bending	7
5. Material required to resist shear forces	10
6. Weight of the wing ribs	11
7. Basic weight of the primary wing box	12
8. Corrections to the basic box weight	13
8.1 Sheet taper and joints in skin-stringer panels and large cut-outs.	13
8.2 Penalties for mountings and connections	14
8.3 Weight penalties due to torsion loads	14
8.4 Aero-elastic effects at high speeds	15
9. Secondary structure weight	16
9.1 Fixed leading edges (fle)	17
9.2 Fixed trailing edges (fte)	17
9.3 Leading-edge high-lift devices (led)	18
9.4 Trailing-edge high-lift devices (tef)	19
9.5 Ailerons (a) and spoilers (s)	20
9.6 Support structure in primary wing box	21
10. Design loads and bending moment relief	21
10.1 The critical fuel load	21
10.2 Computation of the gust load	24
10.3 Weight relief due to fixed masses	24
11. Stress levels and material properties	25
11.1 Lower wing panels	26
11.2 Upper wing panels	26
11.3 Shear stress in spar webs	27
12. Summary and application of the method	28
12.1 Generation of the input	28
12.2 Application of the method	30
12.3 Validation and accuracy	31

13. Conclusions	33
References	34
Figures	37
Appendix: Example calculation of wing weight	46

NOMENCLATURESymbols

A	- aspect ratio ($A = b/\bar{c}$)
	- sectional area of panel structure
b	- span (of wing or center section, see Fig. 2)
b_s	- structural span (see Fig. 2)
C_L	- wing lift coefficient
$C_{L\alpha}$	- wing lift curve slope, $dC_L/d\alpha$
c	- chord length (see Figs. 2 and 10)
\bar{c}	- geometric mean chord ($\bar{c} = S/b$)
c_l	- section lift coefficient
E	- Young's modulus of elasticity
E_t	- tangent modulus of elasticity
F	- shear force
	- efficiency factor of compression panel
$f(\lambda)$	- taper ratio dependent factor of proportionality (eq. 51)
G	- shear modulus
g	- acceleration due to gravity
I_1, I_2, I_3	- non-dimensional integrals for computing bending moment, panel weights and shear material weight
I_z	- bending moment of inertia of cross section
K_g	- gust alleviation factor (eq. 67)
k	- factor of proportionality for weight components
L	- wing lift
	- distance between ribs, measured along elastic axis
M	- (bending) moment
	- Mach number
N_e	- total number of wing-mounted engines
n	- load factor ($n=L/W$)
P	- panel normal load per unit width
q	- dynamic pressure ($q = \frac{1}{2} \rho V^2$)
R_c	- cantilever ratio
r	- inertia relief factor due to masses
S	- reference wing area
\bar{t}	- max. thickness of profile section
t	- height (of spars)
	- mean wing thickness
U_{de}	- derived gust velocity (EAS)
V	- true airspeed
V_C, V_D, V_{MO}	- design airspeeds (EAS)
W	- aircraft All-Up Weight (AUW)
	- weight (component)
Y	- lateral axis
y, \bar{y}, y'	- lateral co-ordinates (see Figs. 4, 10)

α	- angle of attack
γ	- non-dimensional circulation
Δ	- increment of flap specific weight
δ	- (battered) sheet or skin thickness
η	- non-dimensional lateral co-ordinate
η_t	- bending efficiency factor (eq. 23)
Λ	- angle of sweep (positive for sweepback, negative for sweepforward)
$\lambda, \bar{\lambda}$	- taper ratio (see Figs. 2,10)
μ	- aircraft mass parameter (eq. 67)
ρ	- density of structural material or air
$\sigma, \bar{\sigma}$	- normal (mean) stress
$\tau, \bar{\tau}$	- (mean) shear stress

Indices

a	- aileron(s)
B	- bending
BASIC	- basic, primary wing box
BL	- bending due to lift
C	- design cruise condition (structural)
c	- compression
cp	- center of pressure
cr	- compression, at wing root
cs	- center section
D	- design dive condition (structural)
e	- engines
ea	- elastic axis
F	- fuel
FS	- front spar
fle	- fixed leading edge
fte	- fixed trailing edge
g	- gust
L	- (due to) lift
le	- leading edge
led	- leading edge devices
MO	- Maximum Operating
misc	- miscellaneous
NO	- non-optimum
P	- powerplant installation
PRIM	- primary wing structure
RS	- rear spar
r	- wing root (in plane of symmetry)
ref	- reference value or wing station
rib	- wing ribs
S	- shear action
SEC	- secondary structure
SL	- shear due to lift

ST	- stiffness-associated
s	- spoiler(s)
sc	- structural root chord
slat	- leading edge slat system
tef	- trailing edge flap system
tr	- tension, at wing root
to	- at take-off condition
W,w	- due to wing mass
1/2	- mid-chord line

Acronyms

AC	- Active Controls
AUW	- All-Up Weight
c.p.	- center of pressure
DS	- double slotted
DSF	- double slotted Fowler
EAS	- Equivalent Air Speed
GLA	- Gust Load Alleviation
MLA	- Manoeuver Load Alleviation
MLW	- Max. Landing Weight
MTOW	- Max. Take-Off Weight
MZFW	- Max. Zero Fuel Weight
SS	- single slotted
SSF	- single slotted Fowler
TS	- triple slotted
TSF	- triple slotted Fowler
ZF	- zero (wing) fuel condition

Acknowledgements

Many aspects treated in this report and in particular those in connection with stiffness criteria have been discussed with my colleague prof.dr. A. Rothwell and his usefull advices are fully acknowledged.

I am also thankful to Mrs. A. de Jong for her excellent typing of the manuscript and to Mr. W. Spee for drawing the figures.

1. INTRODUCTION

Much effort has been expended, and reported in the literature, on developing wing structure weight prediction techniques. This is partly because the wing happens to be a component which has a well defined structural role, partly because optimum wing design, which is affected sensitively by structural weight variations, forms a very significant subject of preliminary design.

Early wing weight prediction methods were of purely statistical nature and included only simple relationships between wing structure weight and some of the most significant design parameters. Those methods can be of some use then the conceptual designer has to base a weight prediction on scarce data. If, for example, only a wing gross area S is available, a purely statistical approach is to simply plot the wing weight for existing and comparable aircraft versus wing area. A similar typical result will be, for subsonic transport and executive jets:

$$W_w = 17 bS \left(\frac{MZFW}{MTOW} \right)^{1/2} \quad (N) \quad (1)$$

The application of such a purely statistical method (Table 1) shows that the results are sometimes remarkably good, but errors of up to 20% also occur. Such a result is not significantly better than, for example, the rule-of-the-thumb that wing structure weight is approximately 12% of the Maximum Take-Off Weight (MTOW). Although improved statistical methods have been developed in the past, they did not lead to significantly improved predictions for individual aircraft projects, and the main objection of having no indication of sensitivity to parameter variation remained valid.

During the 1950's M.E. Burt (Ref. 7) and F. Shanley (Ref. 8) published weight prediction methods based on elementary strength/stiffness considerations, augmented by experimental results and statistical data. Their approaches enabled weight engineers not only to develop more accurate and design-sensitive results, but they also paved the way to the 'station analysis' methods.

Those methods do not aim at a closed-form expression for the wing weight, but they rely on a computational procedure where the amount of material required to resist bending and torsion at a number of selected spanwise locations is determined numerically. The primary wing box weight is thus found from integration along the span. The contributions of secondary structure (flaps, slats, ailerons, etc.) are finally estimated on a basis of statistics. An example of such a procedure can be found in Ref. 24. It contains an important extension in the sense that lifetime requirements are incorporated, which have a large influence on the allowable stress levels. The approach is based on simple beam theory, but an extension to Finite Element analysis methods seems a logical next step.

Unfortunately, the increasing amount of detailed information required as input for modern, computerized weight prediction methods, does not stimulate their application in preliminary design, particularly when sensitivity studies are required of the effects on overall aircraft characteristics of geometric and parametric variations. For that purpose the combined analytical - empirical methods can still be useful, provided the following facilities are incorporated:

- * It is possible to consider the use of alternative materials;
- * the method can be readily adapted to technologies such as Active Controls;
- * incorporation into modern Computer-Assisted Design systems is foreseen.

The present report describes the development of a wing structure weight prediction that satisfies the above conditions. Although the basic derivation is not totally new, it contains a number of elements that are lacking in existing methods. Although the method yields results with satisfactory accuracy, as shown by the worked examples, the primary objectives are flexibility, unambiguity and robustness. Instead of producing a single formula, the present method provides estimations for the primary subparts of a wing structure. This enables the user to make intermediate checks with data for existing aircraft. If necessary these terms can be judiciously corrected - on the basis of these numbers - to allow for likely deviations, such as special structural configurations or different technology or material application. The baseline is 1980 + technology.

Aircraft	MTOW (kN)	Wing Weight (kN)		
		estimated*	actual	error, %
Airbus A300/B2	1343.6	188.43	196.31	- 4.0
Airbus A340	2487.0	295.32	340.85	- 13.4
BAC 1-11/300	387.0	38.60	42.90	- 10.0
Cessna Citation II	59.16	6.793	5.730	+ 18.5
Boeing 727-100	711.8	75.89	79.02	- 4.0
Boeing 737-200	513.8	39.79	47.21	- 15.7
Boeing 747-100	3158.4	446.15	384.35	+ 16.1
Fokker F-28 Mk 4000	315.8	30.22	33.28	- 9.2
Lockheed 1011-1	1912.8	224.59	210.86	+ 6.5
McD.Douglas DC-9/30	480.4	40.60	50.71	- 19.9
McD.Douglas MD-80	622.8	60.95	69.22	- 11.9
McD.Douglas DC-10/10	2024.0	250.46	217.92	+ 14.9
McD.Douglas DC-10/30	2468.9	252.74	261.83	- 5.3

*Using equation (1)

Standard deviation 12.8%

Table 1: Estimated vs. actual wing weight for jet transports, using a very simple prediction method.

2. WEIGHT SUBDIVISION, GEOMETRY AND METHODOLOGY

For the aircraft category under consideration, subsonic transport and executive aircraft - to be certificated in the airworthiness requirements JAR 25 (and FAR 25) - the wing is generally built up from the subparts depicted in Fig. 1.

All loads on the wing will be ultimately concentrated in the primary box structure, generally consisting of upper and lower stiffened skin panels, a front and a rear spar beam, ribs and a center section inside the fuselage. It is assumed that distributed forces act only outside the fuselage and their resultants are transferred into the fuselage structure at the wing-to-fuselage bulkhead. Although the center section is often unswept, the geometry will be idealized by assuming that the complete primary box has a constant sweep angle between the wing tip and the aircraft plane of symmetry (Fig. 2).

The structural principles assumed are as follows.

- 1) The structure is a statically determined equivalent system:
 - * Bending is absorbed only by the stiffened skin panels and the spar flanges, while the stiffeners are 'battered' with the cover plates to an equivalent plate thickness (δ). Simple beam theory is used for the analysis.
 - * The shear force loads are transmitted by the spar webs, again using an equivalent thickness.
 - * Torsional loads will not be taken into account explicitly, but the box will be checked in a simplified fashion for sufficient torsional stiffness and, if necessary, locally strengthened, mainly in the outer wing.
 - * The ribs support the coverplates, transmit shear loads and introduce concentrated forces into the wing box.
- 2) Only maneuvering and gust loads are considered as the determining cases.
- 3) The emphasis is on accurately predicting the panel loads at the wing root, since the bending moment is usually maximum at the root. However, variation of the material required in lateral direction will be calculated and integrated analytically.
- 4) Stress levels will be obtained from the most important failure criteria and types of construction, taking into account materials characteristics. For quick estimating purposes a statistical method will be presented.
- 5) The 'idealized' theoretical (minimum required) weight will be corrected with so-called non-optimum corrections, which are intended to account for practical deviations from theory, e.g. due to non-tapered skins, splices, joints, opening, access panels, etc.
- 6) Secondary structure weight is estimated for each category separately, using statistical data and functional parameters as input.

Typical wing spar and panel surface design conditions for a large transport aircraft in Fig. 3 illustrate that manoeuvre and gust loads determine most of the primary box structure weight. For the present example (of a swept-back wing) parts of the outer wing are sized by the control loads due to aileron deflection, therefore some attention will be paid to torsional stiffness requirements.

3. THE BENDING MOMENT DUE TO LIFT

The bending moment at any lateral wing station (distance y from plane of symmetry, Fig. 4) is built up from contributions of the wing lift, the distributed mass of the wing structure and fuel, and bending moment contributions of concentrated masses, e.g. wing-mounted powerplants, undercarriage, etc.

In this paragraph only the basic bending moment due to wing lift will be considered; corrections for bending moment relief due to mass terms will be treated in par 9. The bending moment due to lift is obtained from integration of lift contributions outboard of wing station y :

$$M_{BL}(y) = \int_y^{b/2} \frac{y' - y}{\cos \Lambda_{ea}} dL(y') \quad (2)$$

The lift contribution $dL(y')$ is at the elastic axis (ea) and it has therefore been assumed that the aerodynamic pitching moment on each element has a negligible bending moment component at high load factors. The lift distribution is defined by means of a generalized circulation function γ ,

$$\gamma \hat{=} \frac{c_l c}{C_L \bar{c}}, \text{ with } \bar{c} \hat{=} S/b \quad (3)$$

Hence the lift contribution at station y' can be written as follows:

$$dL(y') = \frac{nW}{2} \gamma d\eta', \text{ with } \eta' \hat{=} \frac{y'}{b/2} \quad (4)$$

and the bending moment due to lift is:

$$M_{BL}(y) = \frac{nW}{2} \frac{b_s}{2} \int_{\eta}^1 \gamma' (\eta' - \eta) d\eta' \quad (5)$$

The structural span is equal to:

$$b_s = \frac{b}{\cos \Lambda_{ea}} \quad (6)$$

Ignoring initially the presence of the fuselage, we find the bending moment at the centerline:

$$M_{BL} (y=0) = \frac{nW}{2} \frac{b_s}{2} \int_0^1 \gamma' \eta' d\eta' \quad (7)$$

Since by definition the resulting lift on one wing half acts at the center of pressure (cp), its location is defined by

$$\eta_{cp} = \frac{\int_0^1 \gamma' \eta' d\eta'}{\int_0^1 \gamma' d\eta'} \quad (8)$$

and the bending moment distribution may also be written as:

$$M_{BL} (y) = 1/4 nW \eta_{cp} b_s I_1(\eta) \quad (9)$$

where the bending moment function $I_1(\eta)$ is defined as follows:

$$I_1(\eta) = \frac{\int_0^1 \gamma' (\eta' - \eta) d\eta'}{\int_0^1 \gamma' \eta' d\eta'} \quad (10)$$

The spanwise distribution of the lift is affected by factors such as:

- spanwise chord distribution,
- wash-in or wash-out,
- wing sweep,
- wing section characteristics,
- interference effects between wing and fuselage and/or engine nacelles,
- compressibility effects.

Moreover, torsion due to aerodynamic loads and bending may affect the lift distribution, especially on swept wings. Some remarks on aero-elastic deformation will be made in par 8.4.

The lift distribution can be computed by means of simple theories, such as (extended) lifting-line theory, or by more complicated methods: vortex-lattice or panel methods. In order to illustrate the use of factor $I_1(\eta)$ we will first consider two well-known elementary lift distributions.

- a) The lift coefficient is everywhere constant and equal to C_L and the wing is straight-tapered (taper ratio $\lambda = c_t/c_r$). The γ - distribution is equal to the chord distribution:

$$\gamma' = \frac{2}{1 + \lambda} [1 - \eta' (1 - \lambda)] \quad (11)$$

Substitution into (8) yields for the lateral c.p. location:

$$\eta_{cp} = \frac{1 + 2\lambda}{3(1 + \lambda)} \quad (12)$$

and the function $I_1(\eta)$ according to (10) becomes:

$$I_1(\eta) = \left[3(1 - \eta)^2 - (1 - \lambda)(2 - 3\eta + \eta^3) \right] / (1 + 2\lambda) \quad (13)$$

This equation has been plotted on Fig. 5 for $\lambda = 0.2, 0.5$ and 1.0 . It is found that $I_1(\eta)$ can be approximated very well by:

$$I_1(\eta) \approx (1 - \eta)^{3 - 2\lambda + \lambda^2} \quad (14)$$

b) For an elliptical lift distribution we have:

$$\gamma' = \frac{4}{\pi} \sqrt{1 - \eta'^2} \quad (15)$$

Substitution into (8) yields for the center of pressure:

$$\eta_{cp} = \frac{4}{3\pi} = 0.4244 \quad (16)$$

The $I_1(\eta)$ function for this case is obtained from substitution of (15) into (10), after integration:

$$I_1(\eta) = \left(1 + \frac{1}{2} \eta^2\right) \sqrt{1 - \eta^2} - \frac{3}{2} \eta \arccos \eta \quad (17)$$

Fig. 5 shows that this function is very similar to the previous case, and can be accurately replaced by:

$$I_1(\eta) \approx (1 - \eta)^{2.4} \quad (18)$$

This result is identical to eq. (14) for $\lambda \approx 0.35$, a value resulting in a near-elliptical lift distribution for straight-tapered wings.

The bending moment given by eq. (9) can be used for calculation of the wing panel loads. Since the function $I_1(\eta)$ has been found to be relatively independent of the lift distribution, the problem has been transferred to the determination of η_{cp} . For straight wings at low speeds, a well-known assumption is to take the mean value of a chord-proportional and an elliptic loading, resulting in:

$$\eta_{cp} = \frac{2}{3\pi} + \frac{1 + 2\lambda}{6(1 + \lambda)} \quad (\Lambda_{ea} = 0) \quad (19)$$

Wing sweep can be accounted for by adding .00035 per degree of sweepback of the quarter-chord line.

4. MATERIAL REQUIRED TO RESIST BENDING

A typical wing cross section perpendicular to the elastic axis is depicted on Fig. 6. The upper and lower stiffened skin panels carry the bending moment by means of panel loads, leading to compressive and tensile stresses. The maximum value of these stresses, caused by the bending due to lift are given by:

$$\sigma(y) = \pm \frac{M_{BL}(y)t(y)}{2I_z(y)} \quad (20)$$

where it has been assumed that the neutral axis is midway between the upper and lower surface. The bending moment of inertia $I_z(y)$ can be obtained by replacing the wing panels lower(skin + stiffeners) by an equivalent skin with equivalent thickness $\delta(y)$, at an effective distance equal to $\eta_t t(y)$, with

$$\eta_t \hat{=} 2 \frac{I_z(y)}{t(y)^2 A(y)} \quad (21)$$

where $A(y)$ is the panel cross-sectional area, which is obtained from (20) and (21):

$$A(y) = \frac{M_{BL}(y)}{\eta_t t(y) |\sigma(y)|} \quad (22)$$

The efficiency factor η_t may be obtained from a drawing of the wing cross section. If this is not available, it may be estimated from:

$$\eta_t \approx \frac{1}{3} \left[1 + (t_{FS}/t)^2 + (t_{RS}/t)^2 \right] - .025 \quad (23)$$

or simply by assuming $\eta_t \approx 0.8$.

The basic weight of two upper or lower skin panels is:

$$W = 2\rho g \int_0^{b_s/2} A(y) dy \quad (24)$$

where ρ denotes the material specific density.

Substitution of (9) and (22) yields for the total weight required to resist bending, for constant η_t :

$$W_{BL} = \frac{1}{2} nWb_s \frac{\eta_{cp} b_s/2}{\eta_t t(y=0)} \left[\frac{\rho g}{\sigma_t(y=0)} I_{2t} + \frac{\rho g}{\sigma_c(y=0)} I_{2c} \right] \quad (25)$$

where the integrals I_2 for the lower surface (tension, t) and the upper surface (compression, c) are defined as follows:

$$I_2 = \int_0^1 I_1(\eta) \frac{\sigma(y=0)}{\sigma(y)} \frac{t(y=0)}{t(y)} d\eta \quad (26)$$

This integral can be evolved as follows:

a) Lower panels

The theoretical minimum weight is obtained by assuming that the tensile stress is constant in spanwise direction, hence:

$$I_{2t} = \int_0^1 \frac{I_1(\eta)}{t(y)/t(y=0)} d\eta \quad (27)$$

The ratio of profile thickness depends on the variation of the chord length and on the spanwise variation of t/c . It is found, however, that incorporation of a constant t/c ratio is generally satisfactory. Moreover, the use of various lift distributions, treated in par. 2, practically invariably results in:

$$I_{2t} \approx 0.36 \quad (28)$$

b) Upper panels

The allowable compressive stress is usually considered proportional to the square root of the structural index, for constant tangent modulus:

$$\sigma_c \div \left(\frac{\text{panel load per unit width}}{\text{rib distance}} \right)^{1/2} \div \left(\frac{P}{L} \right)^{1/2} \quad (29)$$

or, for constant ratio of the wing box chord to the wing chord and constant rib distance,

$$\sigma_c \div \left(\frac{M_{BL}}{t(y) c(y)} \right)^{1/2} \quad (30)$$

For constant t/c ratio in spanwise direction, it is found that

$$I_{2c} = \int_0^1 [I_1(\eta)]^{1/2} d\eta \quad (31)$$

Similar to the case of the lower surface panels, there appears to be little variation of this integral for various load distributions. A good average value is:

$$I_{2c} \approx 0.45 \quad (32)$$

Equation (25) has been derived for a linearly decreasing wing thickness between root and tip, while also the presence of the wing/fuselage interconnection has been ignored. The following modifications of the method allow for these effects.

First of all the cantilever ratio R_c is introduced:

$$R_c = \frac{\text{structural span}}{\text{root thickness}} = \frac{b_s}{t_r} \quad (33)$$

Since the normal load on the wing is taken out at the wing/fuselage interconnection, it is more appropriate to use the structural span of the wing outboard of this root section and divide it by the thickness at this same location, t_{cs} (see Fig. 3). Furthermore one finds on many aircraft a pronounced decrease in the t/c ratio between the wing root and the kink, located at approximately 40% semi-span outboard of the centerline. Since this thickness reduction will increase the panel thickness required, the bending material weight must increase. The following definition of the effective cantilever ratio allows for this:

$$R_c = \frac{b_s - b_{cs}}{2 t_{cs}} \left[\frac{2}{3} + \frac{1}{3} \frac{(t/c)_r}{(t/c)_{0.4}} \right] \quad (34)$$

The theoretical minimum material required to resist bending is now obtained from (25) by substitution of (28) and (32). Neglecting the small effect of the nearly constant bending moment in the center section, we obtain:

$$W_{BL} = 0.36 \frac{\rho g}{\sigma_r} n W b_s R_c \frac{\eta_{cp}}{\eta_t} \quad (35)$$

where the mean stress level at the wing root has been defined as follows:

$$\bar{\sigma}_r = 2 \left(\frac{1}{\sigma_{tr}} + \frac{1}{0.8 \sigma_{cr}} \right)^{-1} \quad (36)$$

Although this result seems rather simple, it is to be noted that the selection of the critical load condition (weight distribution) and the mean stress level have a major effect on the result. These subjects will be treated in paragraphs 10 and 11.

5. MATERIAL REQUIRED TO RESIST SHEAR FORCES

Similar to the bending moment, the shear force due to lift at any spanwise station is obtained from integration of the lift outboard of that station:

$$F_{SL}(y) = \int_y^{b/2} d L(y') \quad (37)$$

This can be evolved into:

$$F_{SL}(y) = \frac{nW}{2} I_3(\eta) \quad (38)$$

where

$$I_3(\eta) \hat{=} \int_{\eta}^1 \gamma' d\eta' \quad (39)$$

The area of shear material required, divided approximately equally over the shear webs, at station y is:

$$A_{SL}(y) = F_{SL}(y)/\tau(y) \quad (40)$$

For the two wing halves the total material required to transfer the wing lift amounts to:

$$W_{SL} = \frac{\rho g}{\tau} nW \frac{b_s}{2} \int_0^1 I_3(\eta) d\eta \quad (41)$$

where the shear stress $\tau(y)$ has been assumed constant. It so happens that the integral in (41) is equal to the lateral co-ordinate of the c.p., hence:

$$W_{SL} = \frac{1}{2} \frac{\rho g}{\tau} n W \eta_{cp} b_s \quad (42)$$

Although the shear forces are transferred into the fuselage at the wing root bulkhead, shear webs will be required in the center section as well to cope with torsional loads. Therefore, the complete structural span has been retained in (42), including the center section.

6. WEIGHT OF THE WING RIBS

Contrary to the wing panel weight, a rational derivation for the weight of ribs is not feasible, since these are designed to fulfill a multitude of functions:

- * transfer of distributed air loads to the spars,
- * stabilizing the panels, in particular under compression loads,
- * transfer of concentrated loads of control surfaces, flaps, undercarriages, nacelles, etc. into the wing box,
- * containment of fuel,
- * transfer of the wing loads into the fuselage.

Since the rib mass is strongly dependent on the detailed (structural) wing design, an analytical approach is precluded. This can be illustrated as follows.

Fig. 7 shows the structural lay-out of a DC-10 wing and the general rib weight per unit chord length. (Ref. 23) Using the data in this reference indicates that general ribs have a specific weight of about 50 N/m² in the outboard wing, and 100 N/m² in the center section, while concentrated load-carrying ribs have a specific weight between 200 and 300 N/m². Although the rib pitch varies between root and tip, the average pitch of about 0.75 m is not very different between the outboard and inboard wing.

Several authors have derived optimum rib distances from considerations of minimum weight for compression panels plus ribs. The general result for the optimum rib pitch has the following appearance:

$$L_{opt} \div t \left(\frac{E}{P} \right)^{1/3} \quad (43)$$

where P denotes the panel load per unit chord and t the profile thickness. Using previous derivations, it follows that

$$L_{opt} = (1-\eta) L_r \quad (44)$$

Clearly this is not a realistic outcome and it must be concluded that in practice the rib pitch is based on other considerations than weight minimization.

The present approach is as follows:

- a) It is assumed that the rib specific weight (weight per unit area) is laterally constant.
- b) Part of the rib weight is based on a constant rib pitch, hence rib weight is proportional to wing chord x thickness x span, or:

$$W_{rib} \div \rho g S \bar{t} \quad (45)$$

c) Another part of the rib weight is based on the assumption that rib pitch is proportional to the mean profile thickness, hence:

$$W_{rib} \div \rho g S t_{ref} \quad (46)$$

where t_{ref} is a (constant) statistical reference value. It is found from statistics that a satisfactory approximation for the general rib weight is:

$$W_{rib} = k_r \rho g S \left(t_{ref} + \frac{t_r + t_t}{2} \right) \quad (47)$$

with $k_r = 0.5 \times 10^{-3}$ and $t_{ref} = 1.0$ m. This weight includes the wing-to-fuselage interconnection (pressure bulkhead) and fuel tank boundaries, but not the various weight penalties for support structures, to be treated in par. 8.2.

7. BASIC WEIGHT OF THE PRIMARY WING BOX

Up to now we have only considered the bending due to lift. However, a significant reduction in the bending moment is due to the inertia forces on the wing structure, on the internal fuel load and on any concentrated masses mounted to the wing (e.g. engines, nacelles, undercarriage). Formally this can be taken into account by introducing an inertia relief factor r . Assuming that the same load relief factor applies to the wing panels and the shear webs, we obtain the basic "theoretical" minimum weight by addition of equations 35, 42 and 47.

It is also noted that the constant 0.36 in eq. 35 can be compared to the case of a parabolic distribution of the material between the wing tip and the root, for which this constant amounts to 1/3. Thus, the basic weight is written as follows,

$$W_{BASIC} = \frac{1}{3} \frac{\rho g}{\sigma_r} r n W b_s \eta_{cp} \left(\frac{1.08}{\eta_t} R_c + 1.50 \frac{\bar{\sigma}_r}{\tau} \right) + k_r \rho g S \left(t_{ref} + \frac{t_r + t_t}{2} \right) \quad (48)$$

where R_c is defined by (34). If the shape of the box cross section is known, η_t can be determined from (23), or else $1.08/\eta_t = 1.35$. The factor r will be further analyzed in par. 9.

Equation (48) shows very clearly the effect of aircraft size on wing weight. Comparing wings with the same shape (i.e. constant R_c), for aircraft with different design weights, it is observed that the most important weight contribution as a fraction of the design weight increases with the structural span b_s . Similarly, the rib weight increases proportional to the third power of the linear dimensions; for constant wing loading W/S part of the rib weight fraction increases proportional to the wing thickness.

These unfavorable 'square-cube law' effects are well known; several factors are helpful in counteracting them:

- a) The mean stress level $\bar{\sigma}_r$ is generally lower for the upper (compression loaded) wing panel (see par. 11.2), but its value increases with loading intensity.
- b) For small transport aircraft the wing loading is usually lower than for large aircraft.
- c) The ultimate load factor n for large aircraft is usually based on manoeuvre loads, hence $n = 1.50 \times 2.50 = 3.75$. For smaller aircraft with lower wing loading the gust loads are frequently critical, resulting in a higher ultimate load factor.
- d) The inertia relief due to the distributed fuel load is usually more significant for large aircraft due to their large fuel loads.

8. CORRECTIONS TO THE BASIC BOX WEIGHT

Assuming that the weight of the main wing box has been determined by assuming a maximum stress level in bending for every cross section, we then have to obtain the weight of a complete and practical structure by allowing for

- inability to obtain the optimum cross section at all stations;
- joints, both major and local;
- strengthening around cut-outs;
- mountings for engines, undercarriages, etc.;
- wing-to-fuselage connection;
- weight penalties due to various loads and stiffness requirements;
- miscellaneous influences, e.g. errors due to severe idealization of the structure, general contingencies for safety purposes, etc.

These effects can not be considered analytically and therefore they should be taken into account on the basis of existing data collected for as many manufactured aircraft as possible. These are of necessity of a very approximate nature and may have to be adapted to specific wing configuration; they are often referred to as non-optimum weight.

8.1 Sheet taper and joints in skin-stringer panels and large cut-outs.

The amount of material required to withstand the bending loads varies along the span. Manufacturing and cost effectiveness restrictions do not allow a continuous adjustment of the sheet thickness and stringer shape; in many structures these adjustments take place in steps. However, each time the sheet thickness is adjusted a joint is required. It is obvious that there is an optimum number of adjustments, i.e. a number of changes in sheet thickness at which the total mass of sheets and joints is minimal.

The introduction of linearly tapered sheets and the application of integrally stiffened panels reduces this weight penalty. The proposal made in Ref. 8 for constant sheet thickness, must therefore be considered as conservative.

Since the major part of this weight penalty is related to the surface area of the wing box rather than to the primary box weight, a tentative estimate is obtained by assuming that some extra thickness is required for the skin panels and shear webs:

$$\Delta W_{NO} \approx \rho g S (1 + 2\bar{t}/c) \delta_{NO} \quad (49)$$

where \bar{t}/c denotes the mean profile thickness/chord ratio. The non-optimum extra thickness δ_{NO} can be set at 10^{-3} m (one millimeter) for typical built-up structures, but this value can be halved for integrally machined skin-stringer panels. It should also be noted that for wings with large cutouts for inspection holes and many manufacturing joints a much higher value for δ_{NO} will be required.

8.2 Penalties for mountings and connections

The wing-fuselage attachment weight penalty includes the additional rib weight, the fuselage-attachment and other hardware on the wing. Assuming the wing box to be continuous through the fuselage, this contribution typically amounts to about 0.1% of the MTOW.

The main undercarriage attachment weight penalty is caused by the associated wing cutouts, doublers and fittings, plus the additional rib and door weight. Although this weight depends to some extent on the landing impact load, which in turn is affected by the impact load factor and the landing weight, a fair approximation for "normal" impact velocities is 0.4% of the MLW. This penalty should obviously be left out for fuselage-mounted undercarriages, and appropriately corrected for large transports with additional undercarriages centrally mounted to the fuselage.

For wing-mounted engines the powerplant support structure (e.g. pylon attachments) will locally increase the rib weight. The following is based on scanty statistical data:

$$\Delta W_{NO} = 0.025 (1 + 0.2N_e) W_P \quad (50)$$

where W_P denotes the total weight of the powerplant installation, including the nacelles and pylons, and N_e is the number of engines. There is, however, also a bending moment relief due to the powerplants mass, which will be accounted for as a weight reduction in par. 10.3.

8.3 Weight penalties due to torsion loads

In deriving the primary wing box weight it was assumed that bending loads were the only loads present. However, torsional loads and consideration of torsional stiffness requirements can have a significant effect on the wing weight.

For straight (i.e. unswept) wings with symmetrical profile sections the order of magnitude of the torsional moment at the root is approximately the bending moment divided by the wing aspect ratio. The resulting shear stress in the upper skin is therefore of such magnitude, that it will not affect the allowable compression stress (Ref.39). However, on the tension side the allowable tensile stress will have to be

reduced by up to 10%. The same torsional load will increase the shear load on the front spar and reduce it on the rear spar.

In addition to this load is the torsion due to profile camber, achieving its maximum value at the design diving speed, generally with negative sign i.e. nose-down. In the case of a positive load factor this moment reduces the torsion in absolute magnitude, but in case of $n < 0$ it may become critical. There is also a bending moment increase due to torsion, which is caused by the outward displacement of the center of pressure.

Summarizing the effects of torsion on unswept wings, it is found that in general a detrimental effect is present. Since an accurate calculation, however, requires information about pitching moments and a torsional stiffness distribution, it is arbitrarily proposed to account for these effects by reducing the allowable tensile stress at the root (see par. 11.1) by 10% and increase the shear web weight by 20%.

The effect of sweeping the wing backwards is primarily an increase in the torsional load on the wing root due to the backward displacement of the c.p. relative to the wing root. However, this effect counteracts the positive torsional load due to wing lift. The net effect is zero when the a.c. is at the same longitudinal position as the elastic axis of the centersection and in that case only the torsional load due to the wing section pitching moments remain. It can thus be expected that wing weight is minimal for some positive value of the quarter-chord sweepback angle. We take this into account by replacing the sweepback of the elastic axis by the sweepback angle of the 50% chord line and by adding the same weight penalties mentioned for the straight wing.

Another effect of sweepback is the outboard displacement of the c.p., caused by an outboard displacement of the lift distribution. However, a compensating factor is torsion (wash-out) at the tip due to upwards deflection of the wing. This shifts the c.p. inboard on swept-back wings. Both effects are of the same magnitude and tend to cancel each other. We therefore propose to delete the sweep-correction on the c.p. location suggested in chapter 3.

Summarizing, the effects of torsional loads and static deformation can be taken into account as follows:

- * decrease the maximum tension stress by 10%;
- * increase the shear web weight by 20%;
- * use the 50%-chord sweepback angle instead of Λ_{ea} ;
- * delete a sweepback correction on the c.p. of the rigid wing.

8.4 Aero-elastic effects at high speeds

A second but equally important effect to be considered is the avoidance of aero-elastic effects, such as flutter, aero-elastic divergence or aileron reversal. Several authors (eg. Refs. 5 and 13) have derived criteria for the torsional stiffness required in order to avoid these phenomena, which may occur at high values of the dynamic pressure, hence they are based on the use of V_D , the design diving speed (EAS). These criteria are not accurate, but appear to be well suited for pre-design estimates.

Fig. 8 presents a qualitative indication of the critical speeds at which flutter, divergence and aileron reversal occur as a function of the sweepback angle. Positive sweepback has a relieving effect in the flutter and divergence cases, but may prove to be detrimental in the aileron reversal case. Some of the high-aspect ratio swept-back wings have been problematic with regard to aileron reversal and a solution has been found by applying inboard high-speed ailerons. Outboard ailerons have even been left out altogether on the Airbus A-310, for example, and have been replaced by spoilers.

An illustration of the effect of torsional stiffness requirements on the spanwise weight distribution is illustrated in Fig. 9. Curve A indicates the skin plus stringer (equivalent) thickness required to resist bending; curve B is the panel skin thickness. Application of stiffness requirements results in curve C, indicating the spanwise variation of the skin thickness required to provide torsional stiffness, which is often defined in terms of the deformation energy required to obtain a specified torsional deflection at a reference wing station, usually located 70% semi-span outboard from the root.

Since the amount of skin material required to cope with the bending moment is larger at the inboard wing, the skin thickness of the outboard wing can be reduced relative to line C, e.g. according to line D. Adding the stringers finally results in the line A-E which defines the wing structure mass satisfying both bending and stiffness requirements. The hatched area thus defines the weight penalty due to stiffness requirements.

From the foregoing it will be clear that the implementation of these requirements is possible only in case a detailed knowledge exists of the spanwise torsional stiffness variation and such details as the location of the inertia and flexural axes. However, from various references it was concluded that an empirical weight penalty will have the following appearance:

$$\Delta W_{ST} = f(\lambda) \frac{\rho g}{G} q_D \frac{(b \cos \Lambda_{le})^3 (1 - \sin \Lambda_{1/2})}{(t/c)_{ref}^2 (1 - M_D \cos^2 \Lambda_{1/2})^{1/2}} \quad (51)$$

where $\rho g/G = 10^{-6}$ per meter for Al-alloy, q_D and M_D denote the dynamic pressure and the Mach number at the design diving speed, resp., and "le" refers to the wing leading-edge. The ratio $(t/c)_{ref}$ refers to the wing station at 70% semi-span outboard from the root (see Fig. 2). The factor $f(\lambda)$ is estimated at 0.05 for taper ratio's between 0.30 and 0.80. Typical weight penalties according to (51) are between 2 and 5 percent of the wing weight.

9. SECONDARY STRUCTURE WEIGHT

The secondary structure, contributing a major part (25 to 30%, typically) of the wing weight, generally consists of the following items:

- leading and trailing edge structure;
- high-lift devices at the trailing and/or leading edges;
- control surfaces.

Additional features may be present, such as winglets, external undercarriage bays and fillets at the wing/fuselage interconnection. Since very little information is available on their weight, these items will not be considered here.

9.1 Fixed leading edges (fle)

The only design load on fixed leading edge structures is aerodynamic surface pressure, since the surface panels are generally not designed to carry any part of the wing box bending and torsion loads. The basic parameter for the leading edge weight is the wetted area, which is of the order of 2.5 times the projected area. For a minimum gauge thickness of 0.8 mm, an Al-alloy skin weights approximately 56 N/m^2 . Accounting for ribs and support structure by means of a factor $4/3$, a minimum weight of 75 N/m^2 is obtained. This figure appears to be correct only for the lightest transport aircraft; a more satisfactory relationship is found from statistical data:

$$W_{fle}/S_{fle} = 75 k_{fle} \left(1 + \sqrt{W_{to}/10^6} \right) \quad (\text{N/m}^2) \quad (52)$$

The factor k_{fle} accounts for the strengthening of the leading edge structure to support the movable slats or Krüger flaps:

$$\begin{aligned} k_{fle} &= 1.0 & : & \text{no l.e. devices} \\ k_{fle} &= 1.4 & : & \text{l.e. devices present} \end{aligned}$$

It must be realized that the location of the front spar has an appreciable effect on S_{fle} . Although a more forward location will reduce the leading edge weight, it will also increase the primary structure weight, resulting in a lower efficiency factor η_t (eq. 23). One may therefore either use actual values of η_t and S_{fle} , or statistical values, e.g. $\eta_t = 0.8$ and $S_{fle}/S = 0.18$.

9.2 Fixed trailing edges (fte)

The fixed trailing edge section completes the aerodynamic contour of the wing and provides supporting structure for the control surfaces and flaps. On large transport aircraft it consists of honeycomb skin panels, control surface hinge support ribs, intermediate supports, flap tracks and spanwise auxiliary beams. On wings with appreciable sweepback, part of the landing gear support structure (see par. 8.2) is also provided by this trailing edge structure.

The specific weight of trailing edge structures appears to be affected primarily by the type of high-lift devices at the trailing edge. Using the same approach as for the fixed leading edge, the following result was found for Al-alloy structures:

$$W_{fte}/S_{fte} = 60 \left(1 + 1.6 \sqrt{W_{to}/10^6} \right) + \Delta \quad (\text{N/m}^2) \quad (53)$$

with $\Delta = 0$: single slotted flaps
 $\Delta = 45$: double slotted flaps
 $\Delta = 105$: triple slotted flaps

The trailing edge projected area S_{fte} depends to a large degree on the location of the rear spar, the presence of a kink in the trailing edge and the mechanical design of the trailing edge flaps. In the case of Fowler flaps S_{fte} can be quite large, although the presence of spoilers, inboard ailerons and/or lift dumpers reduces this area. Therefore, a statistical figure for S_{fte} cannot be given and the designer should estimate S_{fte} (as a fraction of the gross wing area) from a preliminary lay-out drawing or from similar aircraft.

9.3 Leading-edge high-lift devices (led)

The following categories of leading-edge devices are found on transport aircraft:

- fixed slots,
- droopnoses,
- slats,
- Krüger flaps.

The first two categories are aerodynamically less efficient (except for very thin wings) and therefore only slats and Krüger flaps will be considered.

Slats are primarily stressed for normal forces, since they experience large suction forces per unit area. The minimum skin thickness is at least 1.6 mm because the slat nose is to protect the wing from rain erosion and hail damage. Closely spaced ribs are required to transfer the high aerodynamic pressure loads; there are heavy ribs where the actuator supports and tracks are located. The tracks are usually made of high strength steel or titanium to react the very high bending loads when slats are extended.

The specific weight of slats is therefore quite high, but less sensitive to the aircraft size as compared to the leading edge weight. For Al-alloy material (e.g. 2024-T3) the following correlation was found:

$$W_{slat}/S_{slat} = 160 \left(1 + 0.7 \sqrt{W_{10}/10^6} \right) \quad (N/m^2) \quad (54)$$

Slat chords are usually between 15 and 25% of the local chord; the higher percentage applies to the outboard wing. Since slats are not always fitted over the full leading-edge span, a statistical estimate of S_{slat} is not appropriate.

Krüger flaps are predominantly used on the inboard part of sweptback wings. Aerodynamically they perform in the same way as slats, but they are less efficient. Fixed-geometry Krüger flaps are simple and light structures compared to slats, generally made of one piece of aluminium, magnesium or composite material. The Boeing 747 uses a variable-camber Krüger flap of deformable glass fiber. The specific weight of Krüger flaps shows a large variation due to the variety in retraction mechanism. However, since their application is restricted and the absolute weight is small compared

to the wing weight (less than 1%), it is satisfactory to assume a specific weight of about 220 N/m^2 for conventional material, referred to the platform area (not extended).

It is to be noted that all specific weights mentioned for leading edge devices refer to the projected area and are including flap track and support weight, but excluding actuators and control devices.

9.4 Trailing-edge high-lift devices (tef)

There are many types of trailing-edge flaps used to increase the maximum lift coefficient. For transport aircraft the older types, split and plain flaps, are now virtually obsolete and most systems use slotted flaps, the number of slots varying between one and three.

A distinction can also be made between slotted flaps and Fowler flaps. Aerodynamically these categories are similar, but Fowler flaps increase the lift by means of a considerable chord extension. Furthermore, some flaps feature a fixed geometry, e.g. a double slotted flap with fixed vane. Others have variable geometry, resulting not only in a rearward motion of the entire flap, but in addition the flap segments are deflected and extended relative to each other, resulting in a flap chord extension up to 35%, combined with flap camber.

It is found that, from the weight point of view, flaps have to be categorized as follows:

SS	:	single slotted
DS	:	double slotted
TS	:	triple slotted
SSF	:	single slotted Fowler
DSF	:	double slotted Fowler
TSF	:	triple slotted Fowler

Slotted flaps have different systems for deflection, varying between simple, fixed hinged support, to complicated four-bar linkages or flap tracks. Fowler flaps feature long support tracks, which are highly loaded. Weight estimating methods which use only the flap loading as the essential parameter, frequently result in a large scatter for long-travel flaps, since the loading of the flap tracks is not taken into account.

The following characteristics have, for a given flap configuration, an effect on flap weight.

- The flap size, mainly in terms of the flap projected area in the nested position, S_{tef} . All other things being equal, the flap load is proportional to this area.
- The flap design speed V_F : loads are proportional to $\frac{1}{2} \rho V_F^2$ or to V_F^2 when using equivalent design speeds.
- The lifting effectiveness, which may be expressed in terms of the increase in lift coefficient at constant angle of attack. Obviously, the flap configuration and deflection angle have a major effect on this.
- The flap thickness/chord ratio, which can be quite small for Fowler flaps mounted on high-speed wings, since they must be retracted below the trailing edge structure.

- e) The number of flap segments per wing panel. Sanders (Ref. 17) introduces this parameter in the weight prediction, indicating that for single slotted flaps the weight increases with the number of segments, while the opposite is true for Fowler flaps.
- f) The sweep angle of the rear spar.
- g) The effect of sonic flap loading on wings with flaps close to the engine exhaust.

If all factors mentioned above are accounted for in the flap weight prediction, the results are generally disappointing. A r.m.s. error of about 20% is the best result that can be achieved, which is unfortunate, because trailing-edge lift devices can have a weight of up to 20% of the wing weight. In the following empirical approach these influences have been indirectly accounted for. It is evident that the required C_L -max value and V_{EF} are strongly dependent on the MTOW, so that a statistical correlation exists between the flap specific weight and the MTOW.

In the author's opinion the most effective approach in preliminary design is one of the following:

- a) Use the specific flap weight of an existing aircraft in the same weight category, with a similar type of high-lift device.
- b) If this is not possible use the following data for Al-alloy flap structures, including flap tracks and supports, but excluding actuators and controls:

$$W_{tef}/S_{tef} = 100 k_{tef} \left(1 + \sqrt{W_{to}/10^6} \right) \quad (N/m^2) \quad (55)$$

using the following values for k_{tef} :

SS	: 1.0	-	add 20% for auxiliary t.e. flap
DS	: 1.50	-	fixed front vane
	: 2.0	-	variable geometry
TS	: 2.40	-	variable geometry
SSF	: 1.80	-	add 20% for auxiliary t.e. flap
DSF	: 2.50	-	fixed front vane
TSF	: 2.90	-	variable geometry

These data should not be used outside the following MTOW ranges:

single slotted : $W_{to} = 50$ to 1000 kN

other flap categories : $W_{to} = 200$ to 4000 kN

Trailing edge flaps usually have chords between 25% and 35% of the local wing chord; they extend to 60-70 percent of the span. If no details are available, a statistical mean value can be taken for S_{tef} , e.g. 16% of the gross wing area.

9.5 Ailerons (a) and spoilers (s)

The specific weight of ailerons on transport aircraft does not show a clearly discernable dependance on such parameters as the design diving speed. Statistically the specific weight appears to be a weak function of the aircraft size, in terms of W_{to} :

$$W_a/S_a = 125 \left[1 + 0.5 \left(W_{td}/10^6 \right)^{1/4} \right] \quad (N/m^2) \quad (56)$$

The total aileron area S_a varies generally between 3% and 5% of the gross wing area. Spoilers and lift dumpers appear to have an average specific weight of about 110 N/m^2 ; their total area may amount up to 6% of the wing area.

When details about the size of control surfaces are lacking, the following statistical weight can be used for ailerons plus spoilers:

$$W_{a+s} = 15 S \quad (N) \quad (57)$$

This weight includes balance weights for ailerons, but not support structure and controls.

9.6 Support structure in primary wing box

The provisions for supporting high-lift devices and ailerons result in extra rib weight, for which the following estimates can be made:

flap supports: 5% flap weight

aileron supports: 20% aileron weight

10. DESIGN LOADS AND BENDING MOMENT RELIEF

In the previous chapters basic expressions have been derived for all wing structural weight components. The primary structural weight was obtained from the bending and shear loads in a relatively straightforward manner. The expressions, however, contain the design All-Up Weights (AUW), the ultimate load factor and a bending moment relief factor r which still have to be specified.

Most wing weight prediction methods in the literature specify the "design weight" as the MTOW and the load factor $n_{ult} = 1.5 \times 2.5 = 3.75$. Though for large transport aircraft this may be correct, aircraft of smaller size are often subject to more critical gust loads and the critical flight and loading condition of the aircraft have to be carefully selected. A considerable part of the inaccuracy of existing prediction methods is caused by ignoring this aspect, since the maximum root bending moment is very sensitive to it.

10.1 The critical fuel load

The term rnW in eq. 48 has a direct and proportional impact on a large part of the wing weight. The question arises as to which loading condition (payload, fuel) and flight speed / altitude will result in maximum bending loads, taking into account the relevant airworthiness rules, eg. FAR/JAR 25.343.

We will first look at the root bending moment and how it is affected by fuel wing outboard the structural root (Fig. 10). For a typical fuel tank geometry the bending moment due to lift and fuel mass is:

$$M_{B_r} = \frac{1}{4} b_s n (\eta_{cp} W - \eta_F W_F) \quad (58)$$

where

$$\eta_{cp} = \frac{\text{lateral coordinate of c.p.}}{\text{structural semi-span}}$$

$$\eta_F = \frac{\text{lateral coordinate of fuel c.g.}}{\text{structural semi-span}}$$

Since the AUW is built up from the Zero Fuel Weight (W_{ZF}) and the fuel weight (W_F) we have:

$$M_{B_r} = \frac{1}{4} b_s n \eta_{cp} \left[W_{ZF} + \left(1 - \frac{\eta_F}{\eta_{cp}} \right) W_F \right] \quad (59)$$

For given load factor this moment is increasing with increasing ZFW and - for $\eta_F < \eta_{cp}$ - also with increasing fuel load. This leads to the critical conditions: $W_{ZF} = MZFW$ and $W_F = MTOW - MZFW$, hence:

$$M_{B_r} = \frac{1}{4} b_s n_{ult} \eta_{cp} MTOW \left[1 - \frac{\eta_F}{\eta_{cp}} \left(1 - \frac{MZFW}{MTOW} \right) \right] \quad (60)$$

where

$$\eta_F / \eta_{cp} = \frac{\bar{y}}{\eta_{cp} \frac{b}{2} (1 - b_{cs}/b)} \quad (61)$$

It can be shown that for a straight-tapered fuel tank with $\bar{\lambda} = c_{F2} / c_{F1}$ (see Fig. 10):

$$\frac{\bar{y}}{b_F/2} = \frac{1 + 2\bar{\lambda} + 3\bar{\lambda}^2}{4(1 + \bar{\lambda} + \bar{\lambda}^2)} \quad (62)$$

Taking for the lift distribution a constant c_l in spanwise direction, the c.p. location is:

$$\eta_{cp} = \frac{1 + 2\lambda}{3(1 + \lambda)} \quad (63)$$

From these approximations the ratio η_F / η_{cp} can be resolved. Taking, for example, $\lambda = 0.30$, $b_F / b = 0.70$, $b_{cs} / b = 0.10$ and $\bar{\lambda} = 0.50$ results in $\bar{y} = 0.39 b_F / 2$, $\eta_{cp} = 0.41$, and $\eta_F / \eta_{cp} = 0.745$. For a complete "wet wing", with $\bar{\lambda} = \lambda$ and $b_{cs} = 0$, one finds $\eta_F / \eta_{cp} = 0.82$.

In all cases where the fuel tank stretches from the root chord to some lateral position we find $\eta_F / \eta_{cp} < 1$. However in cases where, for example, the fuel tank is located outboard of the nacelles, the fuel load will reduce the root bending moment and the critical condition will probably be the Zero Fuel condition, assuming that any fuel tank in the wing center section will be flown empty first.

Gust loads can be more critical for bending than manoeuvre loads, since the gust load factor increases with decreasing AUW. Assuming that the design cruising speed V_C (EAS) is critical for gust loads, the load factor is typically

$$n_{gust} = 1 + K_g \frac{1}{2} \rho_{SL} U_{de} V_C S C_{L\alpha} / W = 1 + \Delta n \quad (64)$$

Substitution into (58) indicates that for $\eta_F > \eta_{cp} / (1 + \Delta n)$ any outboard fuel reduces the root bending moment. This will generally be the case, since for gust-critical conditions $1 + \Delta n > 2.50$. Hence the critical situation occurs for $M_{ZF} = M_{ZFW}$ and the critical ultimate bending moment is:

$$M_{B_r} = 0.375 b_s \eta_{cp} \left(M_{ZFW} + \frac{1}{2} K_g \rho_{SL} U_{de} V_C S C_{L\alpha} \right) \quad (65)$$

From these results it can be concluded that weight relief due to fuel is only important for the case of manoeuvre-critical loads. It cannot be obtained directly from the root bending moment relief, since bending relief acts only on the wing panel containing fuel, while the fuel load is distributed proportional to the primary box chord x thickness, whereas the airload is roughly proportional to the wing chord. Instead of deriving an accurate expression, which would become cumbersome, a simple correction factor on the bending plus shear material is proposed for manoeuvre-critical cases:

$$\left(\frac{\Delta W_{B+S}}{W_{B+S}} \right)_F = - \frac{1 + 3\bar{\lambda}}{4} \left(\frac{b_F}{b - b_{cs}} \right)^2 \left(1 - \frac{M_{ZFW}}{MTOW} \right) \quad (66)$$

For a "wet wing", with $b_F = 0.8 (b - b_{cs})$ and $\bar{\lambda} = \lambda = 0.25$, and with $M_{ZFW} = 70\%$ MTOW this results in a percentage reduction of 8.4%. This is considerably less than the fuel weight relief effect according to Ref. 38, which uses $r = \sqrt{(M_{ZFW}/MTOW)}$, resulting in 16.3% weight relief.

10.2 Computation of the gust load

As stated before, the gust loads are usually critical for the MZFW loading condition. In that case, the airworthiness requirements allow a "structural fuel reserve", which can be neglected for the purpose of weight prediction.

Equation 64 applies to a "sharp-edged" gust speed distribution, assuming a rigid aircraft and only vertical translations are accounted for. To some extent these simplifications are corrected by the inclusion of the gust alleviation factor K_g , which is usually specified in the airworthiness rules as an empirical function of the mass parameter μ ,

$$K_g = \frac{0.88\mu}{5.3 + \mu} \quad \text{where } \mu \hat{=} \frac{2 W/S}{\rho g \bar{c} C_{L\alpha}} \quad (67)$$

with \bar{c} denoting the mean chord S/b and ρ is the atmospheric density.

The lift-curve slope $C_{L\alpha}$ is required for the computation of both μ and the gust-induced airload according to (64). For straight-tapered wings $C_{L\alpha}$ can be calculated according to Ref. 37:

$$C_{L\alpha} \hat{=} \frac{dC_L}{d\alpha} = \frac{2\pi}{2/A + \left[(1 - M^2) / \cos^2 \Lambda_{1/2} + (2/A)^2 \right]^{1/2}} \quad (68)$$

The gust load according to (65) does not contain any correction for the effect of dynamic gust loads. Reference is made to the airworthiness regulations, where in certain cases an increase of the gust load factor is specified for dynamic effects in the order of 15%. However, dynamic gust loads are usually concentrated on the outer wing, for which extra skin thickness has been provided in the form of a weight penalty to cope with stiffness criteria. It is therefore unlikely that this dynamic gust load will have a significant effect on the overall wing weight.

10.3 Weight relief due to fixed masses

Calculation of the weight reduction due to the wing structural weight effect on bending is fundamentally iterative, since the wing weight and lateral mass distribution must be known, which happens to be an outcome of the present method. Since the wing panel equivalent skin thickness decreases in outboard direction, the weight relief is concentrated more inboard than the lift and therefore the bending and shear weight reduction is less than the wing weight fraction. Accounting for this by a 20% reduction, we propose:

$$\left(\frac{\Delta W_{B+S}}{W_{B+S}} \right)_W = -0.80 \frac{\text{wing weight}}{MTOW} \quad (69)$$

It is suggested to assume a conservative 10% for the relative wing weight, or estimate it using eq. 1. In this way an iterative solution is avoided, since a second approximation for the wing weight in (69) is usually not required.

Wing-mounted engines are concentrated masses, resulting in a linear decrease in the bending moment between the powerplants support and the wing root. Outboard of the engines there is no moment relief. It can be shown that the reduction in bending and shear weight is approximately:

$$\left(\frac{\Delta W_{B+S}}{W_{B+S}} \right)_P = -1.50 \sum \frac{\eta_P^2}{\eta_{cp}} \frac{W_P/N_e}{W_{to}/2} \quad (70)$$

where η_P denotes the non-dimensional lateral coordinate of a wing-mounted engine, W_P/N_e the weight per engine of the powerplant plus nacelle plus pylon, while the summation is carried out over one wing half. The factor 1.5 accounts for the difference between a concentrated and a distributed (lift) load. Typical relief factors according to (70) are 0.035 for twin and 0.095 for four wing-mounted turbofan engines. The total powerplants plus nacelles weight in this case is approximately 7.5% of the MTOW. For this aircraft category the powerplant structural support weight is generally negligibly small.

Other fixed masses that may contribute to the wing weight relief are, for example, wing-mounted landing gears and tip tanks. Their effects are generally small enough to be ignored, although the dynamic impact loads on landing due to wing-tip tanks may cause a local weight penalty.

It is finally mentioned that concentrated masses can have a large effect on the flutter characteristics and may therefore contribute to a weight reduction or penalty, depending on their location relative to the elastic axis. Such effects will appear not until extensive flutter analyses have been made, usually downstream of the preliminary design stage.

11. STRESS LEVELS AND MATERIAL PROPERTIES

The all-important factor determining most of the wing weight according to equations 36 and 48 is:

$$\frac{\rho g}{\sigma_r} = \frac{1}{2} \left[\frac{\rho g}{\sigma_{tr}} + \frac{\rho g}{0.8\sigma_{cr}} \right] \quad (71)$$

For most Aluminium-alloy structures used on present-day aircraft the specific weight ρg amounts to $28 \cdot 10^3 \text{ N/m}^3$; for Al-Lithium alloys the value will be 8-10% lower. Stress levels to be used in any practical weight prediction depend to a large degree on the type of material used. This selection is not only a matter of looking at the highest strength and stiffness qualities, but is also based on its proven ability to withstand minor damage in service without endangering the safety of the aircraft. This damage tolerance is of particular concern to avoid that damage caused by fatigue will disastrously weaken the strength of critical components.

11.1 Lower wing panels

The lower wing skins are particularly prone to fatigue through the continuous application - and relaxation- of tension stresses. For this reason the standard material used is an alloy designated 2024-T3, which has very good fatigue resistance. The ultimate tensile stress is approximately 450 N/mm^2 , but to cope with combined tension and shear loading this has to be reduced by at least 10%, e.g. to 400 N/mm^2 . However, for aircraft with critical manoeuvre load this would result in a stress level of $400/3.75 = 106 \text{ N/mm}^2$ in 1-g flight. This is generally considered as too high. For example, a heavily loaded aircraft such as the Boeing 747 uses a maximum tensile stress of 320 N/mm^2 , corresponding to 85 N/mm^2 stress in 1-g flight. It is therefore recommended to use $\sigma_t \leq 350 \text{ N/mm}^2$ for the lower panel at the wing root. For short-range aircraft, which may have ultimate load factors up to 5.0 (gust load) this results in $\sigma_{1-g} \leq 7.0 \text{ N/mm}^2$, which is a good value for obtaining a long crack-free structure up to 40,000 flights.

It should be emphasized that this recommendation applies to conventional materials and structures. The designer should deviate from it if this is felt appropriate. This would also be the case if an exceptionally long service life would be required (see for example Ref. 24).

11.2 Upper wing panels

The upper wing skins have to withstand mainly compression stresses, as the wing flexes upward during flight. The design stress for a conventional skin-stringer structure, with compressive loading intensity P and rib pitch L , is

$$\sigma_c = F \left(\frac{PE_t}{L} \right)^{1/2} \quad (72)$$

where F denotes an efficiency factor for the stiffened skin and E_t is the tangent modulus. The loading intensity P is obtained from the root bending moment,

$$M_{B_r} = \frac{1}{4} n r W \eta_{cp} b_s \quad (73)$$

which has to be divided by the wing thickness and the structural chord c_{sr} of the wing box, measured perpendicular to the elastic axis (Fig. 2):

$$P = \frac{M_{B_r}}{t_r c_{sr}} \quad (74)$$

Where the bending moment is the highest of eqs. 60 and 65. The structural panel efficiency F depends on the details of the structure, such as the type of stringers and the ratio of skin to stringer material. The best practical values obtainable amount to

about 0.8 for Z-stringers and 0.9 for hat-stringers. Assuming the first of these values and taking Young's modulus for E_t , eq. 72 results in:

$$\sigma_c = 0.22 \times 10^6 \sqrt{P/L} \quad (N/m^2), \text{ or: } \rho g / \sigma_c = 0.127 / \sqrt{P/L} \quad (m^{-1}) \quad (75)$$

This applies to stress levels in the elastic range, i.e. up to 270 N/mm^2 for 2024, or up to 450 N/mm^2 for 7075 alloys. For higher stresses the tangent modulus must be used and for 2024-T3 a reasonable approximation is

$$\sigma_c = 7.715 \times 10^6 (P/L)^{1/4} \leq 400 \times 10^6 \quad (N/m^2) \quad (76)$$

A typical maximum compressive stress in the upper wing panel of a Boeing 747 amounts to 400 N/mm^2 . This is about the maximum compression strength of 2024 material, but for the loading of this wing a higher value can be achieved with 7075 material, the more usual choice for upper wing panels. Note that the factor 0.8 in eq. 36 takes into account the reduced panel loading outboard, resulting in lower average compression stress levels.

Although the previous method may be used to determine σ_{cr} , it requires more details of the structure to be known than are usually available. Therefore it is recommended to use for 7075 material:

$$\sigma_{cr} = 400 \times 10^6 (W_{10}/10^6)^{1/4} \quad (N/m^2) \quad (77)$$

Hence the mean value for $\rho g / \sigma_r$ to be used in the calculation of bending material is:

$$\frac{\rho g}{\sigma_r} = 4 \times 10^{-5} \left[1 + 1.10 (W_{10}/10^6)^{-\frac{1}{4}} \right] \quad (m^{-1}) \quad (78)$$

Obviously, in this expression the first term represents the lower surface (tension) and the second term the upper surface (compression). Although eq. 78 generally gives a satisfactory result for conventional Al-structures, the designer may replace it by his own estimates. For Al-Lithium alloy a reduction of about 9% seems feasible, for the same stress levels and good fatigue properties.

11.3 Shear stress in spar webs

Similar to the compression surface, the shear webs can accept stresses which depend on the type of material - 7075 material can accept about 25% higher shear stress than 2024 - and on the load intensity. Similar to compression, the load intensity reduces more outboard, and therefore the ultimate shear stress is varying spanwise. Since many

structural details required are not available and the shear webs constitute a relatively minor contribution, the simple rule has been adopted:

$$\frac{\bar{\tau}}{\sigma} \approx 0.50 \quad (79)$$

In combination with the torsion-induced factor of 1.20 (see par. 8.3), the shear web contribution in eq. 48 amounts to

$$\frac{\bar{\sigma}_r}{\tau} \approx 2.40 \quad (80)$$

12 SUMMARY AND APPLICATION OF THE METHOD

12.1 Generation of the input

The following basic data are required for the calculations:

<u>Design weights:</u>	MTOW; MLW; MZFW
<u>Design speeds:</u>	V_C ; M_C ; V_D ; M_D
<u>Wing geometry,</u> (see Fig. 2)	planform : S ; b ; c_r ; c_t ; Λ_{1e} ; $\Lambda_{1/2}$; profiles : $(t/c)_r$; $(t/c)_{0,4}$; $(t/c)_{0,7}$; $(t/c)_t$; center section : b_{cs} , t_{cs} ; derived : $A = b^2/S$; $\bar{c} = S/b$; $\lambda = c_t/c_r$

Wing tanks : cF_1 ; cF_2 ; b_F

Leading and trailing edges : S_{fle} ; S_{fte}

High-lift devices : S_{led} ; S_{tef} , type

Ailerons and spoilers : S_a , S_s (optional)

From these data the following input is derived

a) Structural span, b_s

This is the total length of the line through the mid-chord points. For straight-tapered wings, disregarding a straight center section:

$$b_s = b / \cos \Lambda_{1/2} \quad (81)$$

It replaces the length of the elastic axis for the reasons explained in par. 8.3. The center section is included.

b) Effective cantilever ratio, R_c

This important ratio is calculated according to eq. 34, which takes into account the presence of the center section as well as spanwise variation in the thickness / chord ratio. In calculating of R_c it must be made sure that one uses the actual structural

thickness of the wing root, instead of using relatively arbitrary definitions of chord lengths and t/c - ratios.

If no detailed data about t/c - variation and the center section geometry are available, the cantilever ratio is simply

$$R_c = \frac{1}{2} b_s / t_r \quad (82)$$

while for straight-tapered wings of constant t/c ratio it can be replaced by:

$$R_c = \frac{A (1 + \lambda)}{4 t/c \cos \Lambda_{1/2}} \quad (83)$$

Since a large part of the basic wing weight is proportional to R_c , this formula clearly illustrates the important effects of aspect ratio, taper ratio and thickness/chord ratio on wing weight.

c) *The lateral position of the center of pressure η_{cp}*

For rigid wings the c.p. location can be obtained from available aerodynamical data or by means of a suitable computational method. Although manoeuvre and gust cases may lead to different values of η_{cp} it is not necessary to account for this. However, compressibility effects and lift losses due to fuselages and wing-mounted nacelles may have a large effect.

A simpler approach is to use eq. (19), leaving out the sweep effect (to account for aeroelastic effects). It is found that for tapered wings η_{cp} is usually close to $4/(3\pi) = 0,4244$, but for $\lambda = 1$ it is about 10% higher.

d) *The design weight and load factor, W and n .*

The bending moment at the root for manoeuvres with MTOW and MZFW is obtained from eq. 60. The ultimate load factor must be used as specified by the airworthiness regulations (usually 3.75 for transport aircraft). A reasonable assumption about the distribution of fuel is necessary.

The root bending moment for the gust case is calculated with eq. 65, using par. 10.2 for the computation of K_g and $C_{L\alpha}$. Obviously, the airworthiness rules must be followed and more accurate data as regards $C_{L\alpha}$ may be used instead of eq. (68).

When the manoeuvre case yields the critical bending moment, a weight reduction ΔW_{B+S} is found from eq. 66. If the gust load appears to be critical no weight relief due to fuel is taken into account. This is conservative, since regulations allow a "structural reserve fuel" to be present.

When it is found that the critical bending moments are quite different, one may consider to reduce maneuver or gust loads (MLA, GLA) by means of active controls, driving the c.p. inboard. Sometimes MLA or GLA is used to reduce the critical bending load to the value of the less critical case. In the present wing weight prediction this can easily be taken into account by assuming the ultimate load nW equal to the non-critical case.

e) *The mass relief factor, r*

Weight relief due to fixed masses is obtained from eqs. 69 and 70 for the wing mass and for wing-mounted engines while eq. 66 is used for fuel mass bending relief only in the case that the manoeuvre load is critical. The relief factor is:

$$r = 1 + \sum \Delta W_{B+S}/W_{B+S} \quad (84)$$

Notice that all values of ΔW_{B+S} are computed as negative values, resulting in $r < 1$.

f) *Mean stress levels, $\bar{\sigma}_r$ and $\bar{\tau}$*

The mean stress levels can be obtained from eqs. 71 and 80. Some additional information is given in par. 11.1 and 11.2. However, in many cases the structural details to compute the allowable stress levels are lacking and one has to rely on an educated guess. It has been found that eq. (78) will give a reasonable approximation for Al-alloy primary structures.

g) *The bending efficiency factor, η_t*

In the case of known values of the front and rear span heights (as a fraction of the local wing section thickness) this factor can be found from eq. 23. Since the wing box section geometry may vary considerably in lateral direction, it is usually necessary to assumed a typical average value, e.g. $\eta_t = 0.8$.

12.2 Application of the method

In accordance with the functional weight breakdown scheme of Fig. 1 we use the primary and secondary weights:

$$W_w = W_{PRIM} + W_{SEC}$$

The primary weight W_{PRIM} relates to the material between and including the front and rear spars, i.e. the top cover, the bottom cover, the spars, the ribs and various attachments (for pylons, undercarriage, etc). This weight includes the centersection and in the present method it consists of three terms:

$$W_{PRIM} = W_{BASIC} + \sum \Delta W_{NO} + \Delta W_{ST} \quad (85)$$

The basic weight W_{BASIC} is the minimum weight of the primary structure required to resist bending and shear loads. It is calculated by means of eq. 48.

The non-optimum weight summarizes penalties for:

- sheet taper and joints : eq. 49
- cutouts, mounting, connections : par. 8.2
- torsion loads: modification of some variables, see par. 8.3.

Eq. 49 requires the input of the specific weight of structural material, (ρ_g) which is $28 \times 10^3 \text{ N/m}^3$ for most Al-alloys.

The weight penalty to allow for stiffness requirements ΔW_{ST} can be estimated by use of eq. 51.

The secondary structure weight summarizes weight components of structural items in front of the front spar and behind the rear spar, plus any miscellaneous weight:

$$W_{SEC} = W_{fle} + W_{fte} + W_{led} + W_{tef} + W_{a+s} + W_{misc} \quad (86)$$

The fixed leading edge weight W_{fle} is obtained from eq. 52, assuming a leading edge area equal to 18% of the cross wing area. If one wishes to study the effect of front spar position on weight the values of both η_t and S_{fle} must be varied, e.g. using eq. 23.

The fixed trailing edge weight W_{fte} depends on the planform geometry and on the type of trailing edge flaps. See par. 9.2, eq. 53.

The weight of leading edge devices for high lift W_{led} can be obtained from eq. 54 for slats and set equal to 220 times the planform area (not extended) for Krüger flaps of conventional material.

The weight of trailing edge flaps W_{tef} can be obtained either by using the specific flap weight for an existing aircraft in the same weight category with a similar flap type, or calculated from eq. 55. The total projected area of the nested flaps should be obtained from a planform drawing or from statistical material, 1/6 of the gross area being a typical value.

The weight of ailerons and spoilers W_{a+s} is readily obtained with the data of par. 9.5.

Miscellaneous weight W_{misc} refers to the support structure mentioned in par. 9.6 and to any additional weight components that have to be input by the user, since no systematic method can be provided for:

- wing-fuselage fairings;
- winglets;
- external undercarriage bays;
- streamline bodies for drag reduction;
- etc.

12.3 Validation and accuracy

The present weight prediction method uses a mixture of rational analysis and statistical information. In particular the selection of the mean stress level at the wing root has a large influence on the results. A validation of the final result has therefore been carried out for several representative transport aircraft in various weight categories.

A worked example for the Boeing 747-100 aircraft in the Appendix demonstrates that the method is easy to apply, provided enough essential information is available. In particular the geometric data, design weights and speeds appear to be important. Since for this aircraft the root bending moment due to the manoeuvre load exceeds the gust

load, the estimation of $C_{L\alpha}$ appears to have no effect on the resulting wing weight. However, the large decrement of t/c in spanwise direction, i.e. from 13.44% at the root to 8% at the 40% span station, increases the bending material by 22.5%. It is also found that due to the definition of the reference wing area the aspect ratio is such that the simple expression eq. 85 results in only a slightly lower value of R_c even though it does not account for thickness variation. The use of the effective cantilever ratio R_c instead of the root thickness chord ratio is considered as an important characteristic of the present method.

The "predicted" wing weight for the B747 is 1.9% higher than the "actual" wing weight specified by the manufacturer. Although this is a satisfactory result, it was decided to repeat this comparison for several other transport aircraft as well. The result is summarized in Table 2, indicating a considerable improvement over Table 1 (page 2).

Aircraft	MTOW (kN)	Wing Weight (kN)		
		computed	actual	error
Boeing 747-100	3158	391.6	384.4	+ 1.9%
Airbus A340	2486	345.0	340.9	+ 1.2%
Fokker F-28 Mk4000	315.8	32.02	33.28	- 3.8%
Cessna Citation II	59.16	5.950	5.730	+ 3.8%

Table 2: Computed vs. actual wing weight for several transport aircraft

Although the small number of aircraft considered does not permit a mean error of prediction to be determined, the table nevertheless indicates that the method yields good results for the size effect. This indicates that the statistical effect of MTOW on various quantities is likely to be satisfactory.

13 **CONCLUSIONS**

A comprehensive method has been developed to predict the structural weight of wings for transport-type aircraft. The objective was to devise a method which is design-sensitive, combining analytical and empirical (statistical) methods. Another objective has been that the user may input various data such as mean compression, tensile and shear stress levels and accurate aerodynamic input, such as the location of the center of pressure and/or the wing lift-curve slope. Instead, the simplified methods presented can be used.

The basic characteristics of the method are as follows:

- a) The wing weight is broken down into functional components (see Fig. 1). Each of these components is estimated in a rational, sometimes semi-statistical way.
- b) The minimum amount of material required in the top and bottom covers to resist the bending load and in the spars to resist the shear load is obtained from analytical integration. The effects of variation in thickness/chord ratio and allowable compressive stresses has been taken into account.
- c) Semi-empirical methods have been developed to account for the weight of ribs, various non-optimum weight penalties and the weight of leading and trailing edge structures, including high-lift devices and control surfaces.
- d) Considerations and methods are given to select the mean stress levels at the wing root. The aircraft size effect on the mean stress level is taken into account by a proposed empirical relation with the MTOW, which is valid for Al-alloy structures. Input of user-selected design stress levels for alternative material applications is also possible.
- e) A procedure is devised to determine the critical loading condition, including the effect of fuel mass relief on the bending moment. Weight relief due to fixed masses is also presented.

The application of the method has been illustrated in a worked example, which shows a satisfactory accuracy in the total wing weight prediction. Prediction errors of less than 4% were found for four representative transport aircraft with take-off weights between 50 and 3500 kN.

REFERENCES

1. Farrar, D.J. : "The design of compression structures for minimum weight". J. of the RAeS, Nov. 1949, pp. 1041-1052.
2. Foss, K.A. and Diederich, F.W. : "Charts and approximate formulas for the estimation of aero-elastic effects on the loading of swept and unswept wings". NACA Report 1140, 1953.
3. Bisplinghoff, R.L. : "Aero-elasticity". Addison-Wesley Publishing Cy., Cambridge Mass. 1955.
Ashley, H.,
Halfman, R.L.
4. Kuhn, P. : "Stresses in aircraft and shell structures". McGraw-Hill Book Cy. Inc., New York, 1956.
5. Broadbent, E.G. : "Aeroelastic problems in connection with high-speed flight". J. of the RAeS, July 1956.
6. Howe, D. : "Initial aircraft weight prediction". College of Aeronautics, Note No. 77, 1957.
7. Burt, M.E. : "Weight prediction for wings of box construction". RAE Report, No. Structures 186, 1955.
8. Shanley, F.R. : "Weight-Strength analysis of aircraft structures". Dover Publications Inc., New York, 1960.
9. Burt, M.E. : "Structural weight estimation for novel configurations". J. of the RAeS, Jan. 1962, pp. 15-30.
10. Anon. : "Endurance of complete wings and tailplanes". ESDU Data sheets-fatigue Vol.1, Sheet E.02.01 RAeS, June 1962.
11. Emero, D.H. : "Wing box optimization under combined shear and bending". J. of Aircraft, March-April 1966, pp. 130- 141.
and Spunt, L.
12. Garrock, C.A. : "Estimation of wing box weights to preclude aeroelastic instabilities" SAWE Paper No. 500, May 1966.
and Jackson, J.T.
13. Sanders, K.L. : "A review and summary of wing torsional stiffness criteria for pre-design and weight estimations". SAWE Paper No. 632, May 1967.
14. Schütz D. : "The fatigue strength of an aircraft upper wing surface". Proc. 9th ICAF Symposium Darmstadt, May 1979.
and Lowak, H.

15. Sewell, R.T. : "Low altitude flight load spectra for light aircraft". National Research Council of Canada, Aeronautical Report LR-495, Ottawa 1967.
16. Coker, B.B. : "Problems in airframe development associated with weight and balance control in heavy logistics transport vehicles such as the C-5A transport". Short course in modern theory and practice of weight optimization and control for advanced aeronautical systems, University of Tennessee, Nov. 1968.
17. Sanders, K.L. : "High-lift devices, a weight and performance trade-off methodology". SAWE Paper No.761, 1969.
18. Clevenger, R.E. : "Preliminary wing loads for transport aircraft".
and Traver, E.W. Douglas Paper 5820, Sept. 1970.
19. Howe, D. : "The prediction of empty weight ratio and cruise performance of very large subsonic jet transport aircraft". Cranfield Report Aero 3, 1971.
20. Howe, D. : "Structural weight prediction". Cranfield Institute of Technology DES903, 1971 (Unpublished)
21. Torenbeek, E. : "Prediction of wing group weight for preliminary design". Aircraft Eng., July 1971, page 16.
22. Schijve, J. : "The accumulation of fatigue damage in aircraft materials and structures". AGARDograph No. 157, Jan. 1972.
23. Marsh, D.P. : "Post-design analysis for structural weight estimation". SAWE Paper No. 936 (Douglas Paper 6021), 1972.
24. Schneider, W. : "A procedure for calculating the weight of wing structures with increased service life". SAWE Paper No. 1021, May 1974.
25. Patterson, R.W. : "Weight estimates for QUIET/STOL aircraft". SAWE Paper No.1001, 1974.
26. Hangartner, R. : "Correlation of fatigue data for aluminium aircraft wing and tail structures". National Aeronautical Establishment, Aeronautical Report LR-582, Ottawa, Dec. 1974.
27. Edwards, P.R. : "Studies in fretting fatigue under service loading
and Ryman, R.J. conditions". Proc. 8th ICAF Symposium, Lausanne, 1975.

28. Gerard, G. : "Handbook of structural stability. Part V. Compressive strength of flat stiffened panels". NACA TN 3785, 1975.
29. Fritz, R.J. : "Method for determining the maximum allowable stress for preliminary aircraft wing design". University of the Witwatersrand, Johannesburg; School of mechanical engineering Research Report No. 72, Jan. 1977.
30. Beltramo, M.N. and Trapp, D.L. : "Parametric study of transport aircraft systems cost and weight". NASA CR 151970, april 1977.
31. Anderson, R.D. : "Development of weight estimates for lifting surfaces with active controls". The SAWE Journal, Vol. 36, April, 1977.
32. Storey, R.E. : "Dynamic loads and airplane structural weight". SAWE Paper No 1153, Los Angeles, 1977.
33. Ramsey H.D. and Lewolt, J.G. : "Design manoeuvre loads for an airplane with an active control system". Proc. of the 20th Structures, Structural Dynamics and Materials Conf.; AIAA/ASME/ASCE/AHS, St. Louis, 1979; Page 456-464. (NASA CP 1795)
34. Toll, T.A. : "Parametric study of variation in cargo-airplane performance related to progression from current to spanloader designs". NASA Technical Paper 1625, 1980.
35. York, P. and Labell, R.W. : "Aircraft wing weight build-up methodology with modification for materials and construction techniques". Grumman Aerospace Corporation, prepared under contract No. NAS2-9805 for NASA, 1980.
36. Wissel, W.D. : "Advanced material application on the European wide body transport aircraft Airbus". SAWE Paper No. 1484, 1982.
37. Torenbeek, E. : "Synthesis of subsonic airplane design". Kluwer Academic Publishers, 1982. ISBN 90-247-2724-3.
38. Shevell, R.S. : "Fundamentals of flight". Prentice Hall Inc., 1983 ISBN 0-13-339093-4.
39. Niu, M.C.Y. : "Airframe Structural Design". Lockheed Aeronautical Systems Cy, CONMILIT PRESS LTD., 1988. ISBN 962-7128-04-X.
40. Udin, S.V. and Anderson, W.J. : "Wing mass formula for subsonic aircraft". J. Aircraft, Vol. 29, No. 4, Page 725-727.

FIGURES

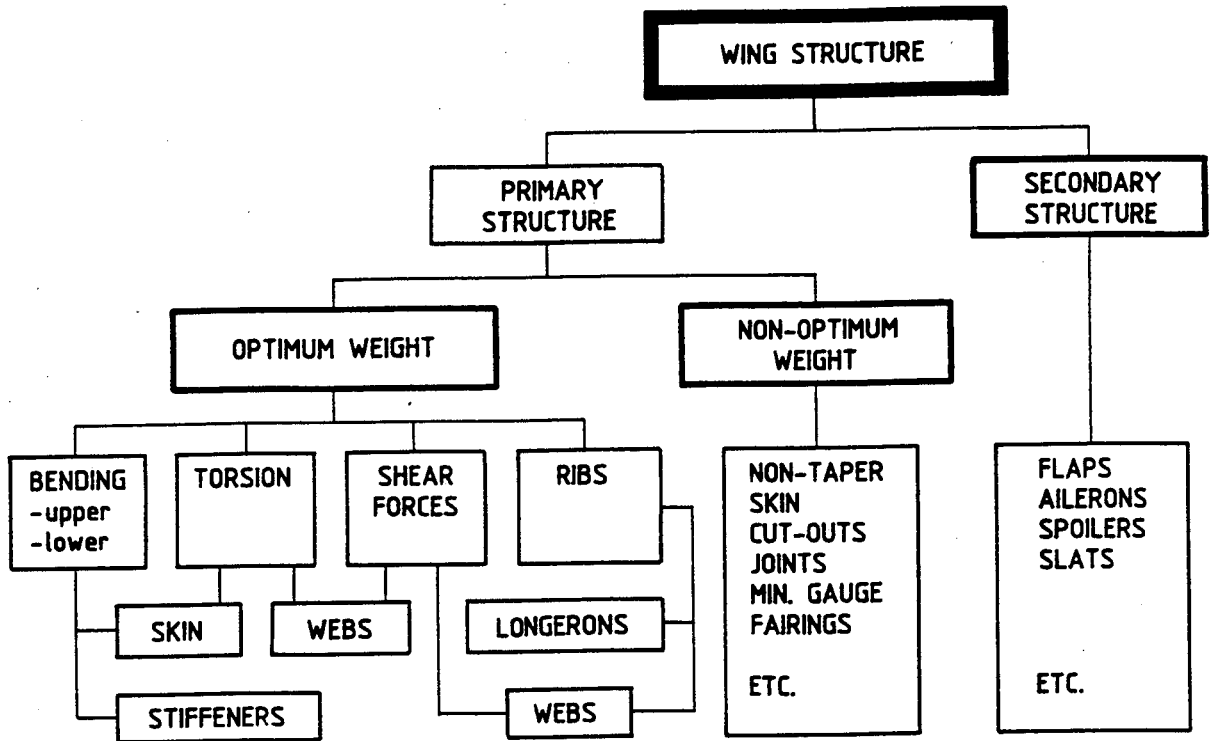


Fig. 1: Subdivision of wing structure and weight contributions.

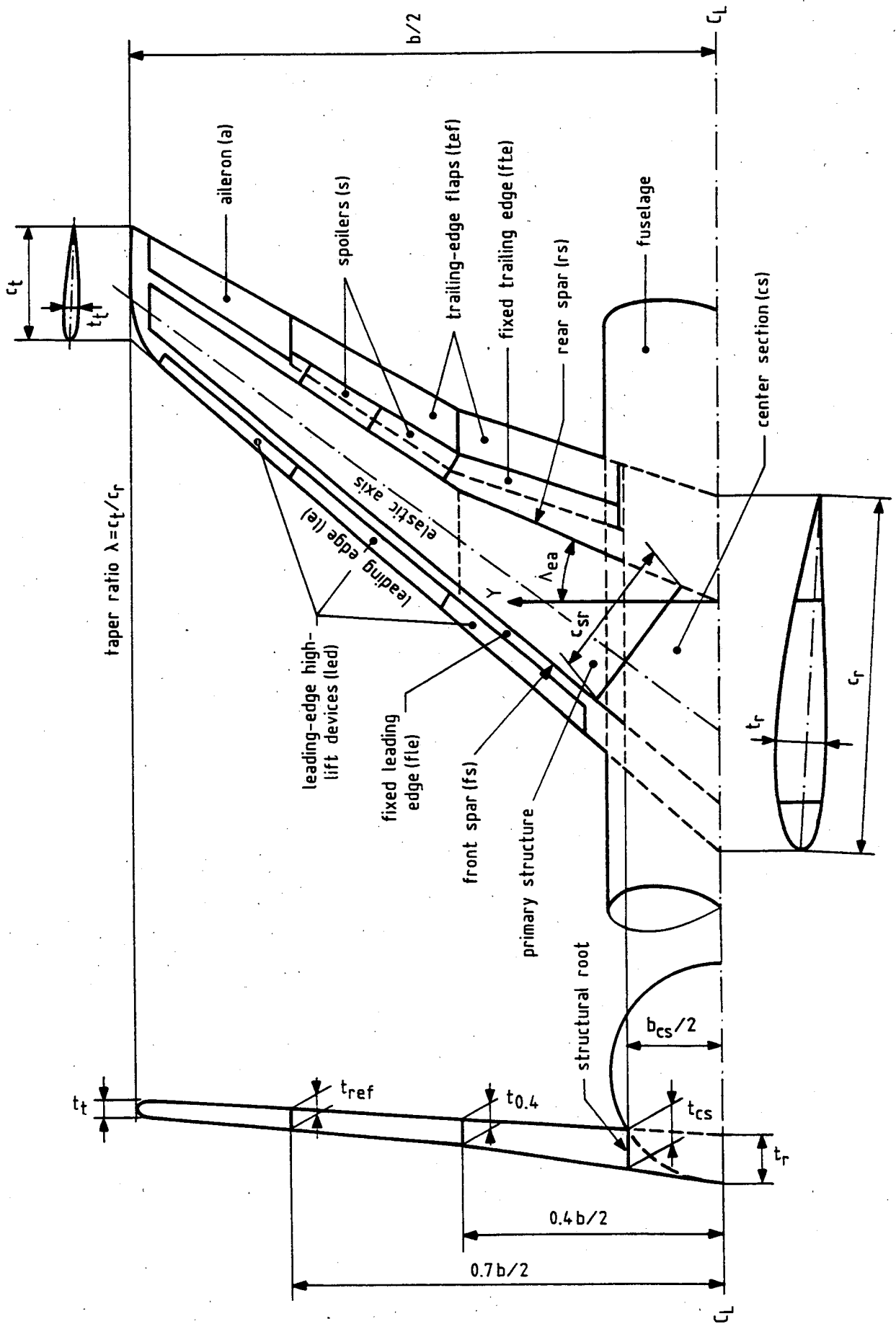
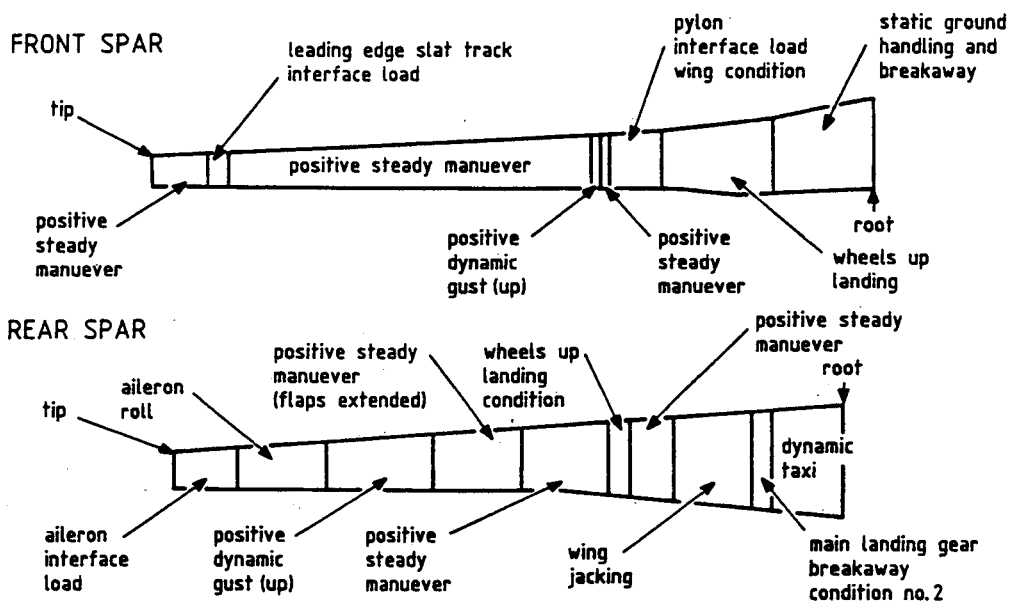
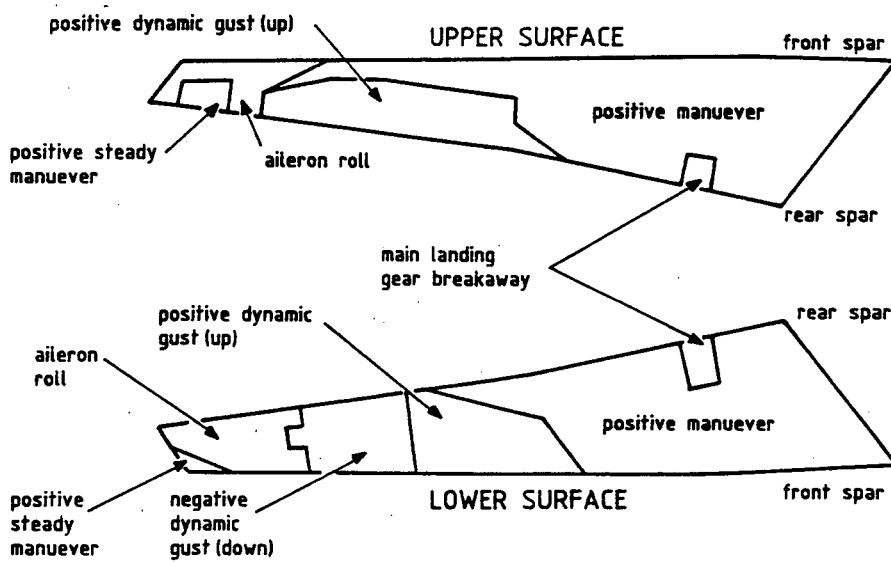


Fig. 2: Wing geometric definitions and nomenclature



Spar design conditions



Panel design conditions

Fig. 3: Typical design conditions for a primary wing structure (Ref. 33)

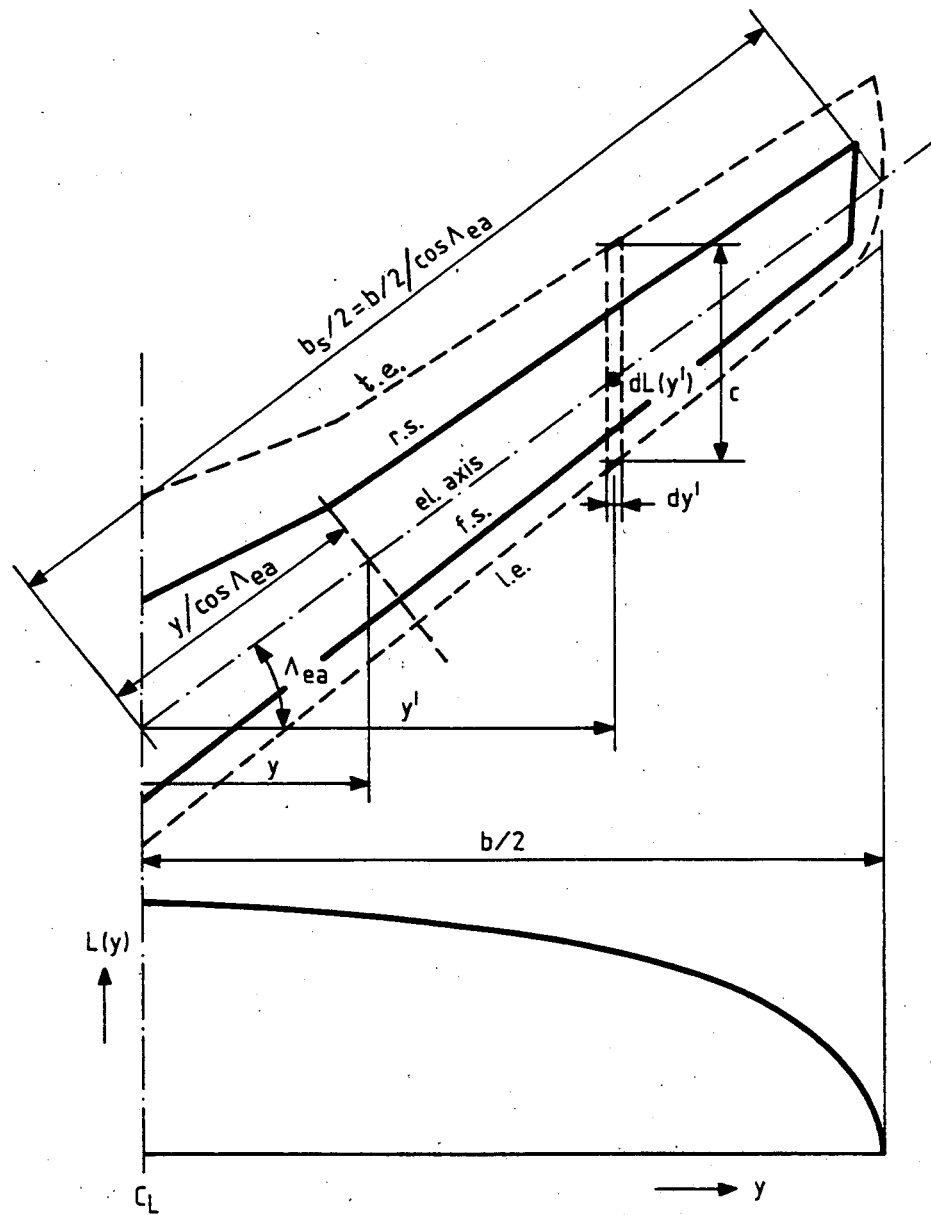


Fig. 4: Nomenclature for calculating the bending moment due to lift.

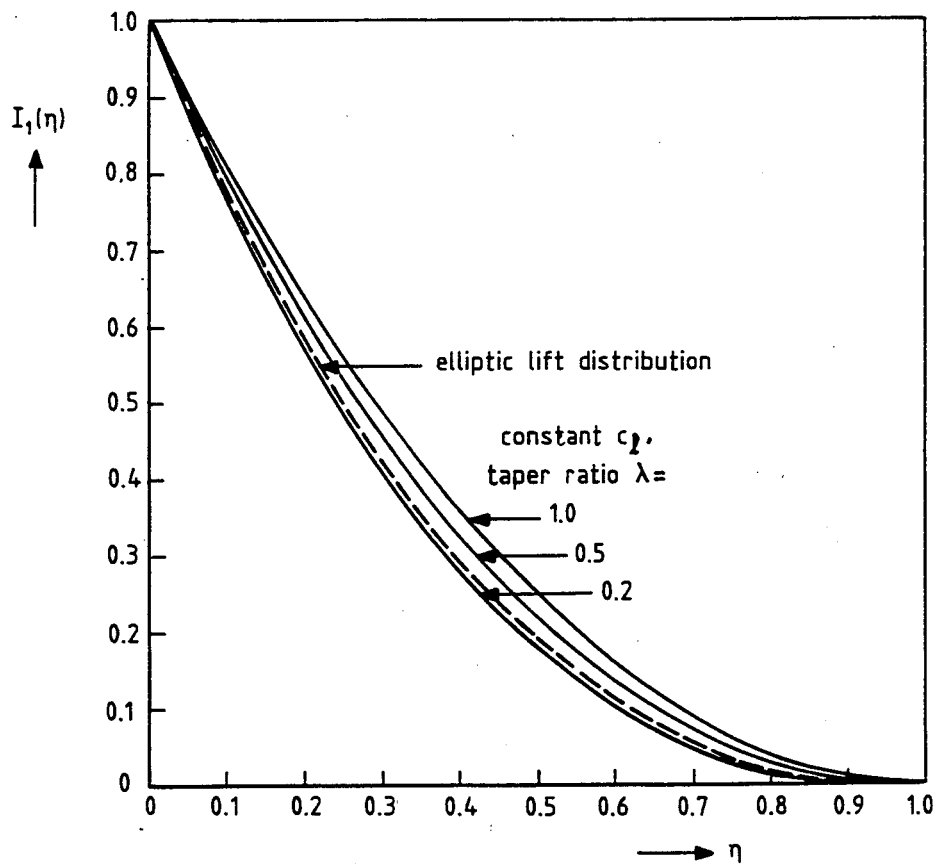


Fig. 5: The bending moment distribution function $I_1(\eta)$ for two elementary lift distributions.

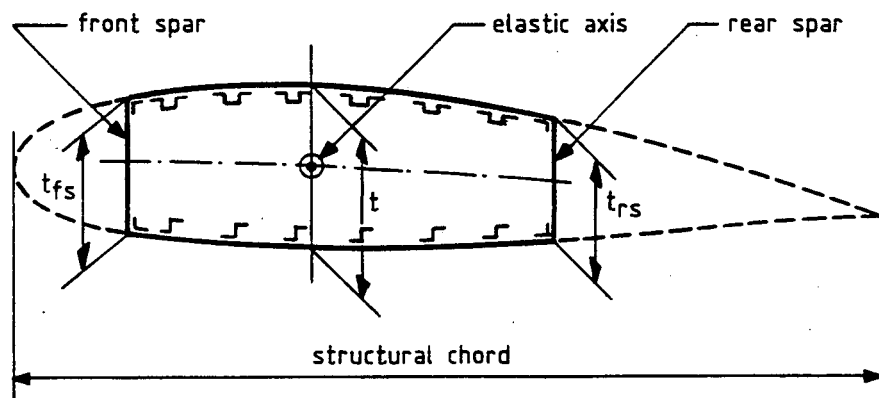


Fig. 6: Typical wing cross section perpendicular to the elastic axis

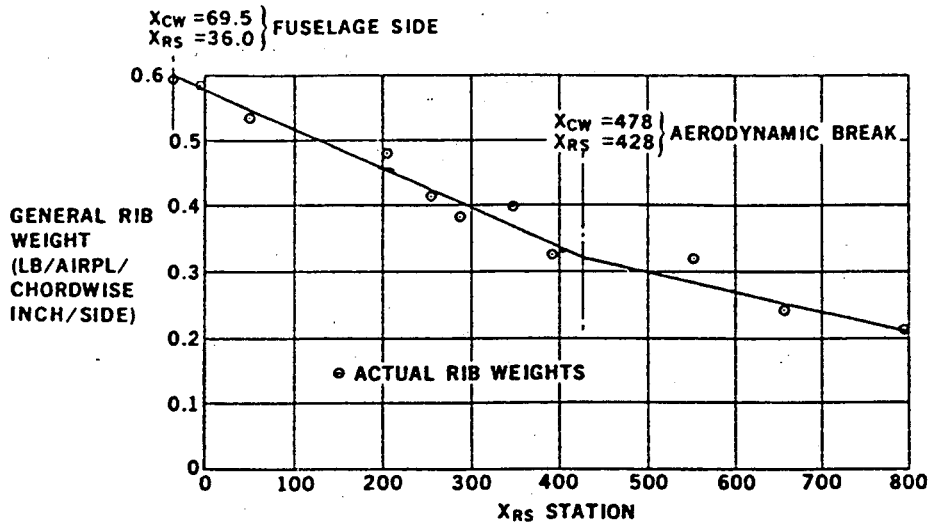
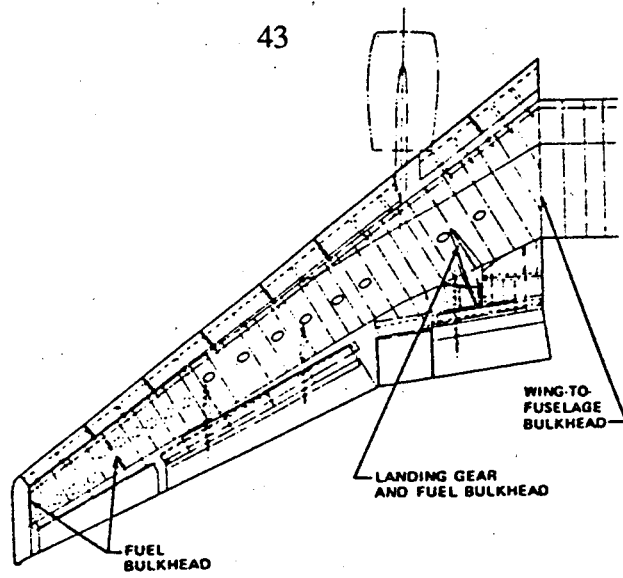


Fig. 7: Wing rib arrangement and spanwise general rib weight distribution for the McDonnell Douglas DC-10/10 aircraft (Ref. 23).

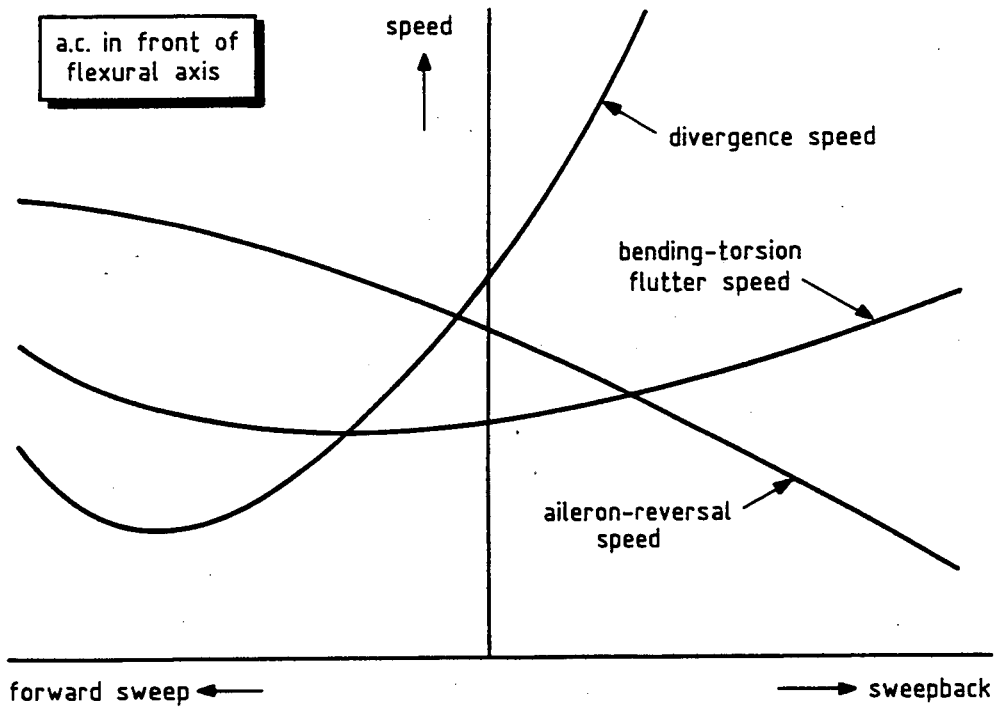


Fig. 8: Influence of wing sweep on divergence, flutter and aileron reversal speed.

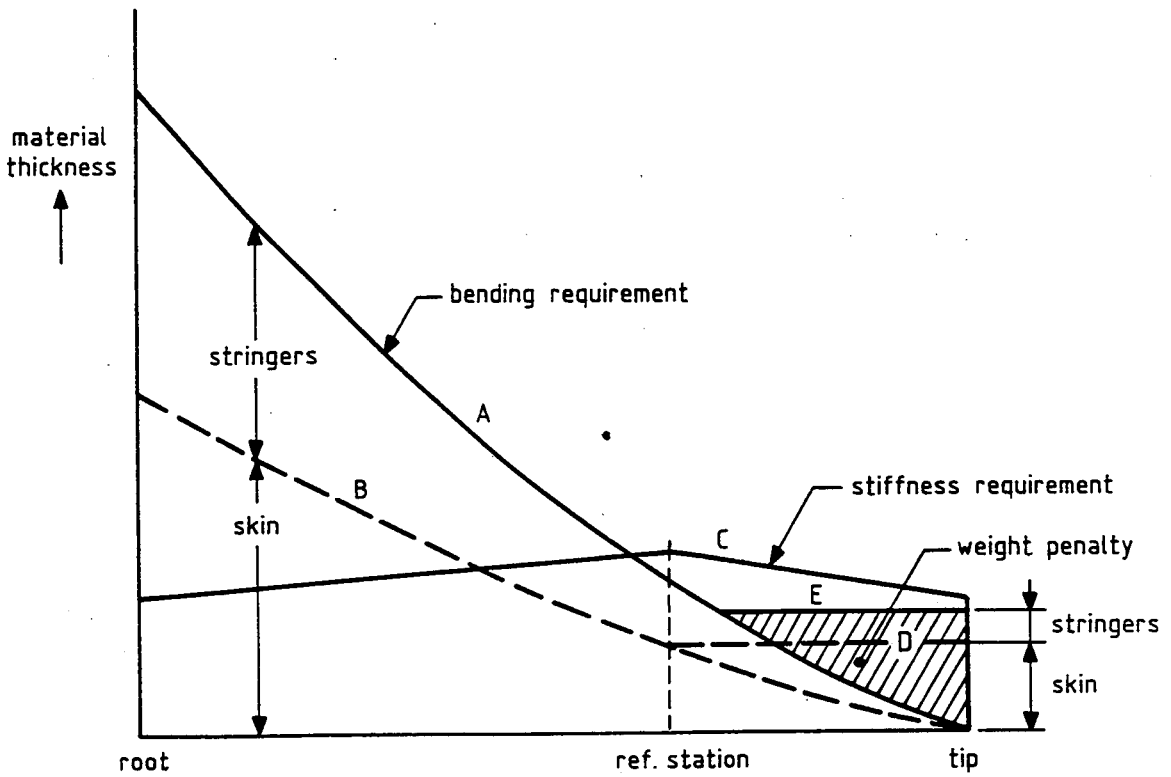


Fig. 9: Material required to resist bending and to provide torsional stiffness.

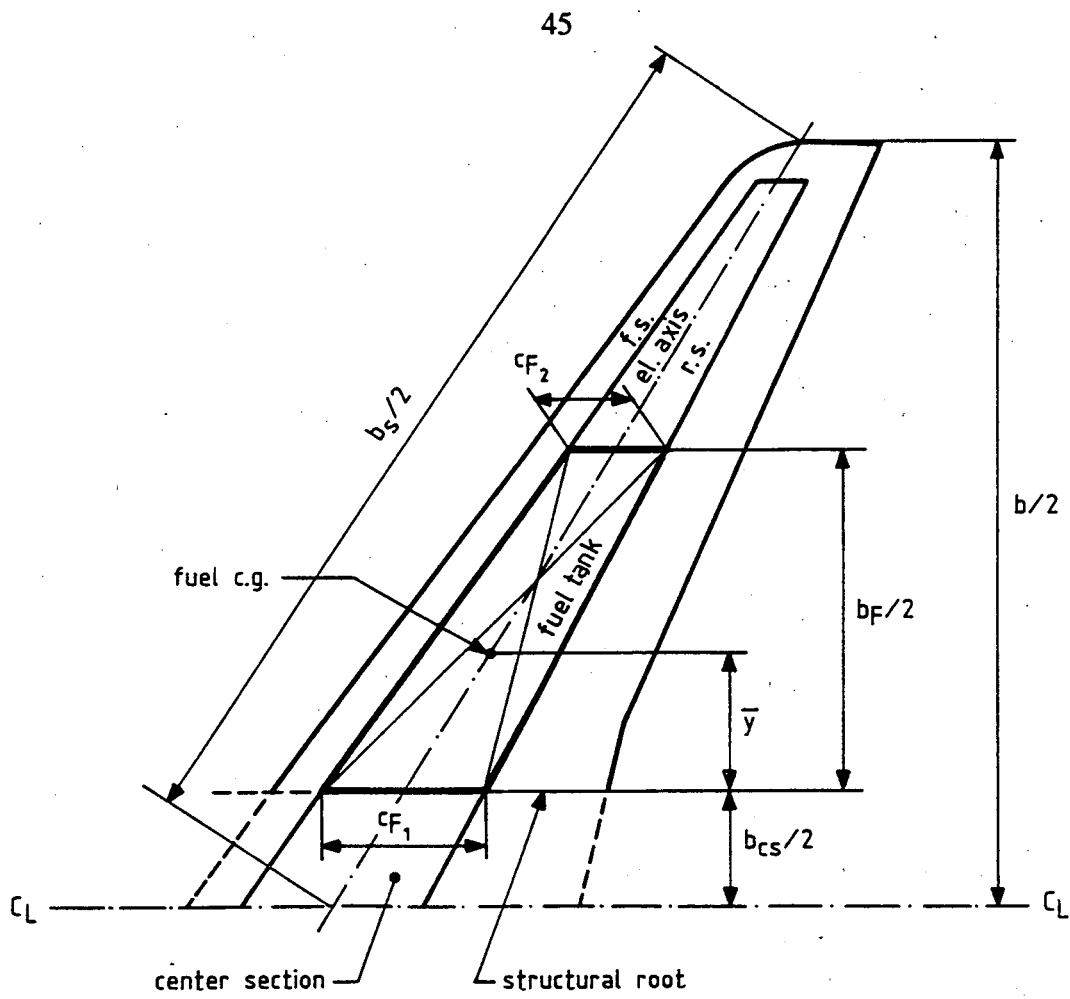


Fig. 10: Fuel tank geometry (see also Fig. 2)

APPENDIX

EXAMPLE CALCULATION OF WING WEIGHT

As an illustration of the present method the wing structural weight will be estimated for the Boeing 747-100. Most of the input was taken from Jane's All the World's Aircraft 1977-1978.

Design Weights

MTOW	= 710,000 lb	(3158.4 kN)
MLW	= 564,000 lb	(2508.9 kN)
MZFW	= 526,500 lb	(2342.1 kN)

Geometry

Reference Area	: S	= 5500 ft ²	(511.0 m ²)
Span	: b	= 195' 8"	(59.64 m)
Mid-chord sweep angle	: $\Lambda_{1/2}$	= 35.3°	
Leading edge sweep angle	: Λ_{le}	= 41.2°	
Root chord (y = 0)	: c_r	= 54' 4"	(16.56 m)
Tip chord (y = b/2)	: c_t	= 13' 4"	(4.06 m)
Aspect ratio	: A	= 6.96	
Taper ratio	: λ	= 0.245	
Center section span	: b_{cs}	= 6.15 m	
Thickness/chord ratio - root	: t/c	= 0.1344	
- 40% span	: t/c	= 0.080	
Thickness at root (y = 0)	: t_r	= 2.225 m	
at y = $b_{cs}/2$: t_{cs}	= 2.00 m	
Taper ratio of wing tank	: $\bar{\lambda}$	= 0.25	

Design conditions

Design cruising speed	: V_C	= 162.5 m/s	(EAS)
Design cruising Mach number	: M_C	= 0.90	
Design dive speed	: V_D	= 229 m/s	(EAS)
Design dive Mach number	: M_D	= 0.97	

Calculation of input data

According to eq. 83 the structural span is $59.64/\cos 35.3 = 73.076$ m.
The cantilever ratio as used in the method is, according to eq. 34:

$$R_c = \frac{73.076 - 6.15}{2 \times 2.00} \left(\frac{2}{3} + \frac{1}{3} \frac{0.1344}{0.08} \right) = 20.524$$

Compared to eq. 85,

$$R_c = \frac{1}{4} \frac{6.96 (1 + 0.245)}{0.1344 \cos 35.3} = 19.75$$

it is surprising that in spite of the large t/c - variation the two definitions are not very different. The reason is that for the Boeing 747 the reference wing area is not based on the present root chord definition.

The lateral position of the center of pressure is estimated from eq. (19):

$$\eta_{cp} = \frac{2}{3\pi} + \frac{1 + 2 \times 0.245}{6 (1 + 0.245)} = 0.4117$$

The wing lift-curve slope according to eq. 68, for $M = 0.90$, amounts to $C_{L\alpha} = 7.03$ per rad. Aerodynamic data available indicate for the complete aircraft a lift curve slope of 0.117 per degree, or 6.70 per rad. The latter value is used for the computation of the mass parameter μ according to (67), for a mean geometric chord $\bar{c} = S/b = 8.568$ m. Since the gust load will be computed for the MZFW condition, we have at 20,000 ft (6100 m) altitude

$$\mu = \frac{2 \times 2.3421 \times 10^6 / 511}{0.65283 \times 9.807 \times 8.568 \times 6.70} = 24.94$$

and the gust relief factor is:

$$K_g = \frac{0.88 \times 24.94}{5.3 + 24.94} = 0.7258$$

In order to determine the critical root bending moment for manoeuvres the lateral coordinate of the fuel must be known. Assuming that only the tanks outboard of the fuselage contain fuel, eq. 62 yields:

$$\frac{\bar{y}}{b_F/2} = \frac{1 + 2 \times 0.25 + 3 \times 0.25^2}{4 (1 + 0.25 + 0.25^2)} = 0.3214$$

Estimating $b_F/2$ equal to 85% of $b/2$, according to (61) we have

$$\eta_F/\eta_{cp} = \frac{0.3214 \times 0.85}{0.4117 (1 - 6.15/59.64)} = 0.744$$

The root bending moment for the manoeuvre load factor $n = 3.75$ is obtained from eq. 60:

$$M_{B_r} = 71.953 \times 10^6 \text{ Nm}$$

For the gust case we apply eq. 65, which yields for a design gust speed of 15,25 m/s:

$$M_{B_r} = 68.965 \times 10^6 \text{ Nm}$$

It is thus concluded that the manoeuvre case is more critical than the gust case.

The mass relief effects are now calculated according to eq. 66:

$$\left(\frac{\Delta W_{B+s}}{W_{B+s}} \right)_F = -0.0974$$

Estimating the wing weight at 12% MTOW, or 3.80 kN approx., the wing weight relief factor according to (69) is equal to:

$$\left(\frac{\Delta W_{B+s}}{W_{B+s}} \right)_W = -0.096$$

Since detailed weight data of the powerplant installation are lacking, we use the relief factor for the powerplant as suggested in par. 10.3: for 4 wing-mounted engines:

$$\left(\frac{\Delta W_{B+s}}{W_{B+s}} \right)_P = -0.095$$

The relief factor thus becomes:

$$r = 1 - (0.0974 + 0.096 + 0.095) = 0.7116$$

The mean root stress level is calculated according to eq. 78:

$$\frac{\rho g}{\bar{\sigma}_r} = 4 \times 10^{-5} \left[1 + 1.10/3.1584^{1/4} \right] = 73 \times 10^{-6} \text{ m}^{-1}$$

Since the wing section geometry varies strongly in spanwise direction and structural details of the primary box are lacking, we assume the efficiency factor $\eta_t = 0.80$. Using the mean shear stress level according to eq. 80, the first bracketed term in (48) amounts to:

$$\frac{1.08}{\eta_r} R_c + 1.50 \frac{\bar{\sigma}_r}{\tau} = 31.3074$$

The first term of eq. (48), representing the basic bending and shear material, amounts to 193.17 kN. The basic rib weight as represented by the second term of (48) amounts to 16.28 kN, for $t/c = 0.08$ at the tip. Hence:

$$W_{BASIC} = 209.45 \text{ kN}$$

According to eq. 49 the non-optimum weight for sheet taper and joints is 17.45 kN, or 8.3% of the basic weight. The penalties mentioned in par. 8.2 are assumed at 0.1% MTOW and 0.2% MLW, resp., since only two of the four main undercarriages are mounted to the wing, or 8.176 kN. Equation 50 yields a weight penalty of 10.76 kN for the engine support structure. In total we get:

$$\Delta W_{NO} = 36.386 \text{ kN}$$

The weight penalty for stiffness requirements, proposed in par. 8.4, uses the dynamic pressure at the design dive speed:

$$q_D = \frac{1}{2} \times 1.225 \times 229^2 = 32,120 \text{ N/m}^2$$

Equation 50 then yields:

$$\Delta W_{ST} = 0.05 \times 32,120 \times 10^{-6} \cdot \frac{44.87^3 (1 - 0.6587)}{0.08^2 (1 - 0.97 \times 0.816^2)^{1/2}} = 0.013 \times 10^6 \text{ N}$$

This stiffness penalty amounts to 3.4% of the wing weight.

The primary wing weight may now be computed:

$$W_{PRIM} = 209.45 + 36.386 + 13.00 = 258.836 \text{ kN}$$

The fixed leading edge weight is obtained from eq. 52; for an estimated $S_{fle} = 0.18 \text{ S} \approx 92 \text{ m}^2$

$$W_{fle} = 92 \times 1.4 \times 75 \left(1 + \sqrt{3.158}\right) = 20,826 \text{ N}$$

The specific trailing edge weight according to (53) is, for triple slotted flaps, 271.6 N/m^2 . The trailing edge area, excluding spoilers, is estimated at 55 m^2 . Hence

$$W_{fte} = 14.938 \text{ kN}$$

According to eq. 54 the specific weight of the slats amounts to 359 N/m^2 and the slat area is 38.35 m^2 . Hence the slat weight is 13.768 kN . For 9.7 m^2 Krüger flap area the weight is approx. 2.134 kN , hence

$$W_{lef} = 15.902 \text{ kN}$$

From eq. 55 the specific weight of the triple slotted flap system is estimated at 805 N/m^2 . For a total nested flap area of 78.7 m^2 the weight is accordingly:

$$W_{tef} = 63.354 \text{ kN}$$

For a specific aileron weight according to (56) of 208 N/m^2 and total aileron area of inboard and outboard ailerons equal to 20.6 m^2 , the aileron weight is 4.285 kN . For a spoiler area of 30.8 m^2 and a specific weight of 110 N/m^2 the spoilers weigh 3.388 kN . Totalling we find

$$W_{a+s} = 7.673 \text{ kN}$$

Finally, the miscellaneous weight is according to par. 9.6

$$W_{misc} = 4.024 \text{ kN}$$

For the secondary wing weight we find in summary:

$$W_{SEC} = 132.717 \text{ kN}$$

The wing weight is accordingly:

$$W_w = W_{PRIM} + W_{SEC} = \underline{391.553} \text{ kN}$$

This is nearly identical to the first approximation that has been used to calculate the wing mass relief factor. Therefore a second iteration is not necessary.

The calculated wing weight compares favourably with the actual wing weight, specified as $86,402 \text{ lb}$, or 384.4 kN . The prediction error is $+1.86\%$.

